HUMAN PICORNAVIRUSES: UNCOATING, ASSEMBLY AND INTERACTION WITH CELLULAR RECEPTORS

SHABIH SHAKEEL

Institute of Biotechnology
and
Department of Biosciences
Division of Genetics
Faculty of Biological and Environmental Sciences
and
Integrative Life Science (ILS) Doctoral Program, Doctoral School in Health Sciences,
University of Helsinki

ACADEMIC DISSERTATION

To be presented for public examination with the permission of the Faculty of Biological and Environmental Sciences of the University of Helsinki in the auditorium 1041 of Biocenter 2, Viikinkaari 5, Helsinki, on April 11th at 12 o' clock noon.

HELSINKI 2014

Supervisors

Docent Sarah J. Butcher, Ph.D.
Research Director,
Structural Biology and Biophysics Program,
Institute of Biotechnology,
University of Helsinki, Finland

Professor Arto Urtti
Centre for Drug Research,
Faculty of Pharmacy,
University of Helsinki, Finland

Reviewers

Dr. José Ruiz Castón
Department of Structure of Macromolecules, Centro Nacional de Biotecnología/CSIC, Madrid, Spain

Dr. Petri Auvinen
DNA Sequencing and Genomics Lab, Institute of Biotechnology, University of Helsinki, Finland

Opponent
Professor David I. Stuart
Division of Structural Biology,
University of Oxford, U.K.

Custodian

Professor Tapio Palva
Division of Genetics, Department of Biosciences, Faculty of Biological and Environmental Sciences,
University of Helsinki, Finland

Thesis committee group

Professor Adrian Goldman
Department of Biochemistry
University of Helsinki, Finland
and
The Astbury Centre for Structural Molecular Biology, University of Leeds, U.K.

Dr. Varpu Marjomäki
Department of Biological and Environmental Sciences,
University of Jyväskylä, Finland

ISBN 978-952-10-9803-1 (paperback)
ISBN 978-952-10-9804-8 (PDF, http://ethesis.helsinki.fi/)
ISSN 1799-7372

Yliopistopaino, Helsinki University Printing House
Helsinki 2014

To PSB

Table of Contents

Original publications

This thesis is based on the following three articles and one unpublished manuscript, which are referred to in the text by their Roman numerals.

I. Seitsonen JJ, Shakeel S, Susi P, Pandurangan AP, Sinkovits RS, Hyvönen H, Laurinmäki P, Ylä-Pelto J, Topf M, Hyypiä T, Butcher SJ. 2012. Structural analysis of coxsackievirus A7 reveals conformational changes associated with uncoating. Journal of Virology 86:7207-15.

II. Shakeel S, Seitsonen JJ, Kajander T, Laurinmäki P, Hyypiä T, Susi P, Butcher SJ. 2013. Structural and functional analysis of coxsackievirus A9 integrin αvβ6 binding and uncoating. Journal of Virology 87:3943-51.

III. Pandurangan AP*, Shakeel S*, Butcher SJ and Topf M. (2013) Combined approaches to flexible fitting and assessment in virus capsids undergoing conformational change. 2014. Journal of Structural Biology 185:427-439.

IV. Shakeel S*, Dykeman EC*, White S*, Ora A, Twarock R, Stockley PG, Butcher SJ. RNA packaging signals dictate assembly in a human picornavirus. (Manuscript)[#]

Author's contribution in each publication:
I. SS performed homology modelling and flexible fitting, analysed and interpreted data from 3-D reconstructions and flexible fitting. This work was presented as a manuscript in JSS's PhD thesis (2011, University of Helsinki). JSS performed cryo electron microscopy and image processing. SS, JSS and SJB wrote the paper.

II. SS planned experiments and performed electron cryo-microscopy, image processing, 3-D reconstructions, tomography, flexible fitting, analysed and interpreted data. SS and SJB wrote the paper.

III. SS planned experiments; setup a generalised processing pathway for complex macromolecular structure fitting, performed homology modelling, flexible fitting, validation of the models, analysed and interpreted data. All authors wrote the paper.

IV. SS planned experiments, cultured and purified virus, prepared and labelled pentamers, performed electron cryo-microscopy, assisted in processing next generation sequencing data and sequence alignments, analyzed and interpreted data. SS, ECD, SW, RT, PGS and SJB wrote the manuscript.

*These authors contributed equally.
[#]Patent application filed based on this study.

Abbreviations

3-D	Three-dimensional
Å	Ångstrom
CAR	Coxsackie adeno receptor
CCD	Charge-coupled device
CNS	Central nervous system
CPS	Component placement score
cryo-EM	Cryo transmission electron microscopy
cryo-ET	Cryo electron tomography
CTF	Contrast transfer function
CVA16	Coxsackievirus A16
CVA21	Coxsackievirus A21
CVA6	Coxsackievirus A6
CVA7	Coxsackievirus A7
CVA9	Coxsackievirus A9
DAF	Death accelerating factor
DED	Direct electron detector
DNA	Deoxyribonucleic acid
DQE	Dynamic quantum efficiency
EV71	Enterovirus 71
EV-A	Enterovirus group A
FMDV	Foot-and-mouth disease virus
GA	Bacteriophage GA
HPeV1	Human parechovirus 1
HPeV3	Human parechovirus 3
HRV2	Human rhinovirus 2
ICAM1	Intracellular adhesion molecule 1
IRES	Internal ribosome entry site
MP	Maturation protein
MS2	Bacteriophage MS2
NGS	Next generation sequencing
NMR	Nuclear magnetic resonance
PS	Packaging signal
PV1	Poliovirus 1
RGD	Arginine-glycine-aspartic acid
RMSD	Root mean square deviation
RNA	Ribonucleic acid
SCARB2	Human scavenger receptor class B, member 2
SCCC	Segment cross correlation coefficient
SELEX	Systematic evolution of ligands by exponential enrichment
smFCS	Single molecule fluorescence correlation spectroscopy
ss	Single-stranded
STNV	Satellite tobacco necrosis virus
TEM	Transmission electron microscope
TR	Translation repressor

UTR	Untranslated region
VP	Viral protein

ABSTRACT

Pathogenic human picornaviruses are known to cause a wide variety of diseases ranging from mild colds to severe paralysis. In addition to their importance in causing disease, they also serve as models for understanding the basic mechanisms of host-pathogen interactions, virus entry, viral genome release, viral synthesis and viral assembly. In picornaviruses, the majority of the structural and host-cell interaction studies have been conducted on polioviruses and human rhinoviruses. Picornaviruses like coxsackievirus A 7, coxsackievirus A 9 and human parechovirus 1 have not been so well studied because of difficulties in culturing them. Recently, the number of cases reported for infection by these viruses has increased dramatically due to better detection methods, thus making structural studies of these viruses and their interactions with their host cells important in order to understand their mode of infection so that better therapeutics can be designed against them.

I have studied coxsackievirus A 7, coxsackievirus A 9 and human parechovirus 1, which are all pathogenic picornaviruses, in order to understand the mechanism of pathogenesis, tropism, viral entry and assembly for these viruses in particular and for picornaviruses in general. Two studies dealt with determining the structure of coxsackievirus A 7, a *Human Enterovirus A* species for which there was no structural information available at the time when this study was conducted. The genome-filled and empty structure of coxsackievirus A 7 were determined using cryo electron microscopy to sub-nanometer resolution which helped in building pseudo-atomic models for them using homology modelling and flexible fitting. With the help of these models, the majority of the strain variations in the capsid proteins were identified on the

surface of VP1. Such variations are the likely cause of differences in pathogenesis and tropism between strains. Furthermore, superimposition of these models showed that the capsid underwent a conformational change on RNA release. In the process, generalised methods for optimising and comparing results from flexible fitting were developed. The next structural study elucidated the interaction of coxsackievirus A 9, a *Human Enterovirus B* species, with a cellular receptor. Integrins were found to bind sub-stoichiometrically to the capsid using electron cryo-tomography (cryo-ET). Asymmetric reconstruction indicated that this was probably due to steric hindrance. The affinity of this interaction was calculated to be 1nM using surface plasmon resonance. Additionally, the conformational changes which occur on its RNA release were quantified. The fourth study explained the importance of viral RNA in picornavirus assembly. Pentameric intermediates of human parechovirus 1 were isolated and used to identify packaging signals in the viral RNA required for capsid assembly using aptamer library screening and next generation sequencing analysis. Poly-U was identified as the common motif for these packaging signals present on the stem or the loop of the RNA secondary structure.

Overall, this thesis gives an insight into many important aspects of host-virus interactions especially the events occurring on viral RNA exit and during its encapsidation. The work in this thesis could be utilized to identify potential targets for antiviral synthesis and also to define general virus assembly principles.

1. INTRODUCTION

1.1 Picornaviruses

There are a large number of icosahedrally-symmetric small, single stranded (ss) ribonucleic acid (RNA) containing animal viruses that belong to the family Picornaviridae. The family consists of seventeen genera which have about 37 species (Adams *et al.* 2013) (http://www.picornaviridae.com/, as on 15.11.2013). They are known pathogens of both human and animals and are associated with several important diseases. The majority of the infections by picornaviruses are transmitted by the oral-fecal route (Yun *et al.* 2008, Baba *et al.* 2012), are asymptomatic or cause mild respiratory infections like the common cold caused by rhinoviruses (Arnold and Rossmann 1990). However, some enterovirus infections e.g. by poliovirus and enterovirus 71 lead to severe diseases like paralysis and meningitis (Chumakov *et al.* 1979, Rastogi *et al.* 1983, Verboon-Maciolek *et al.* 2002). In cloven-hoofed animals, foot and mouth disease is a highly infectious disease caused by foot and mouth disease virus (FMDV). There have been numerous outbreaks of this disease causing great economic loss to the farming industry (Salmon 1903, Henderson 1969, Knight-Jones and Rushton 2013). Picornaviruses are studied not only because of their infections in human and animals but also because they serve as model system for studying various biological processes like replication of RNA (Tuschall *et al.* 1982, Van Dyke *et al.* 1982), apoptosis (Tolskaya *et al.* 1995, Schwarz *et al.* 1998), necrosis (Bozym *et al.* 2011), immune responses (Bedke *et al.* 2012, Howe *et al.* 2012a, Howe *et al.* 2012b), and self-assembly of macromolecules (Chung *et al.* 2010, Li *et al.* 2012, Porta *et al.* 2013). Picornaviruses are even being tested for biopharmaceutical applications to

serve as gene delivery vectors (Jia *et al.* 2002, Kim *et al.* 2012) and as oncolytic agents (Atsumi *et al.* 2012, Miyamoto *et al.* 2012, Liu *et al.* 2013).

1.1.1 Capsid structure

Picornaviruses are composed of the protective protein shells called capsids which keep the encapsidated nucleic acid safe from degradation by nucleases. Among the different common shapes of virus capsids like isometric, rod-shaped helices and pleomorphic, are the small, compact and icosahedrally-symmetric picornavirus capsids (Hogle *et al.* 1985, Rossmann *et al.* 1985, Semler 2002). The picornavirus capsids are also responsible for host cell recognition, viral attachment and capsid entry into the host cells. In addition, capsid proteins aid in the release of viral RNA into the host cells. Picornaviruses have small genomes ranging from ~7000-8500 nucleotides in size (Kitamura *et al.* 1981, Racaniello and Baltimore 1981, Carroll *et al.* 1984, Callahan *et al.* 1985). Thus, they prudently use several copies of the same or similar proteins capable of assembling into a symmetric structure where all subunits occupy the same environment (e.g. icosahedral or helical capsid) as proposed initially by Watson and Crick for viruses with small genomes (Crick and Watson 1956). The proposed theory of Crick and Watson was later improved upon by Caspar and Klug for icosahedrally-symmetric viral capsids with more than 60 subunits (Caspar and Klug 1962). Their 'quasi-equivalence theory' stated that for capsids with more than 60 subunits, each subunit occupies a similar but not identical environment in the capsid. (Caspar and Klug 1962). The triangulation number (T number) describes the number of structural subunits per asymmetric unit (Caspar and Klug 1962). The icosahedral capsid of picornavirus have T=1 (pseudo*T*=3) symmetry which

means that one asymmetric unit of the capsid is made up of 3 similar but not identical proteins (Caspar and Klug 1962, Hogle *et al.* 1985, Rossmann *et al.* 1985, Semler 2002).

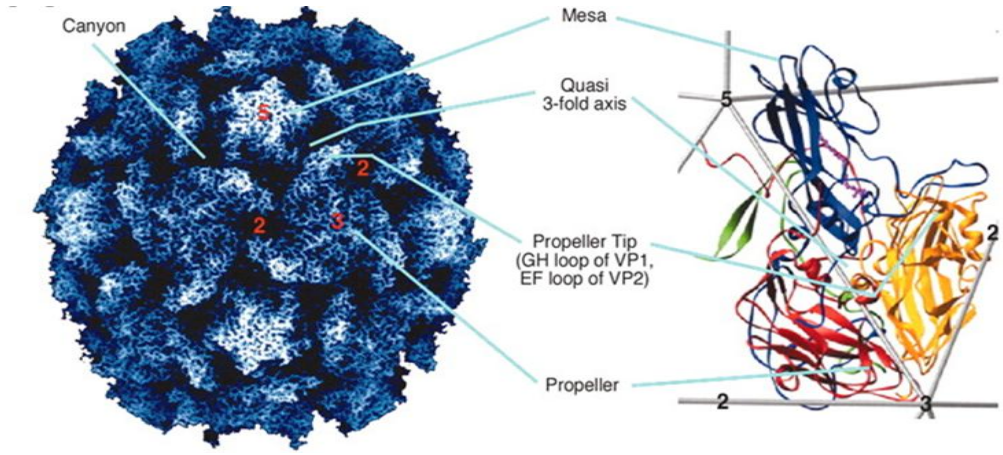

Figure 1. Poliovirus capsid

Adapted from Bubeck D. *et al* Journal of Virology 2005 with permission from American Society of Microbiology. The left panel shows three-dimensional surface representation of a poliovirus capsid. The right panel shows an asymmetric unit of the capsid made of VP1 (blue), VP2 (yellow), VP3 (red) and VP4 (green).

Picornavirus capsids are composed of viral proteins VP1, VP2, VP3 and VP4 (Figure 1 and Figure 2) (Hogle *et al.* 1985, Rossmann *et al.* 1985, Semler 2002) except viruses in the genera *Parechovirus* and *Kobuvirus* where VP0 does not undergo cleavage into VP2 and VP4 (Yamashita *et al.* 1998, Stanway and Hyypiä 1999). These four viral proteins compose one asymmetric unit and five such units make up a pentamer (Semler 2002). Twelve pentamers together

make up a T=1 capsid (Semler 2002). There are five-fold, three-fold and two-fold rotational symmetries found in these capsids (Figure 1) (Hogle *et al.* 1985, Rossmann *et al.* 1985, Semler 2002). VP1 is found around the five-fold vertices whereas VP2 and VP3 are found around the two-fold and three-fold axes of symmetry (Figure 1) (Hogle *et al.* 1985, Rossmann *et al.* 1985, Semler 2002). The small mostly unstructured VP4 is found underneath VP1, VP2 and VP3 (Hogle *et al.* 1985, Rossmann *et al.* 1985, Semler 2002). VP1 protrudes from the capsid surface at the five-fold vertices making a 'mesa' whereas the VP2 and VP3 extend beyond the capsid surface at the three fold symmetry forming a 'propeller' (Figure 1) (Hogle *et al.* 1985, Bubeck *et al.* 2005b). In entero- and rhinoviruses, these features give an impression of a 'canyon' between them (Figure 1) (Hogle *et al.* 1985, Rossmann *et al.* 1985). The depth of the canyon varies among the entero- and rhinoviruses (Semler 2002). The VP3 N-terminus makes an annulus around the five-fold vertices whereas the N-termini of VP1 and VP2 along with VP4 make contact with the RNA (Rossmann *et al.* 1985, Hadfield *et al.* 1997, Hendry *et al.* 1999).

The amino acid sequence identity between VP1, VP2 and VP3 is low e.g. in Poliovirus 1 mahoney strain (UniProt ID: P03300), the sequence identity between VP1 and VP2 is 13.6%, between VP1 and VP3 is 17.4% and between VP2 and VP3 is 15.7% calculated with ClustalW (Larkin *et al.* 2007) (http://www.ebi.ac.uk/Tools/msa/clustalw2/, accessed on 16.11.2013). However, these capsid proteins have a common conserved β-barrel (jelly-roll) structure with four antiparallel β strands on each side (Figure 1) (Rossmann *et al.* 1985). Atomic models of many entero- and rhinoviruses have revealed the presence of a lipid molecule called a pocket factor within the hydrophobic region of the VP1 β-barrel (Hogle *et al.* 1985, Rossmann *et al.* 1985, Filman *et*

al. 1989, Kim *et al.* 1993, Oliveira *et al.* 1993, Muckelbauer *et al.* 1995, Smyth *et al.* 1995, Hadfield *et al.* 1997, Hendry *et al.* 1999, Plevka *et al.* 2013). It is known to give stability to the capsid and its binding site is being exploited as an antiviral target (Plevka *et al.* 2013, De Colibus *et al.* 2014).

1.1.2 Host recognition and interaction

Although the overall structure of picornaviruses is similar (see section 1.1.1) (Hogle *et al.* 1985, Rossmann *et al.* 1985, Acharya *et al.* 1989), they utilize a wide variety of cellular receptors in order to gain entry into the host cells (Greve *et al.* 1989, Mendelsohn *et al.* 1989, Berinstein *et al.* 1995, Jackson *et al.* 2000). The cellular receptors may be proteins, for example, integrin αvβ6 for FMDV and coxsackievirus A9 (CVA9) (Jackson *et al.* 2000, Heikkilä *et al.* 2009), sugar moieties (e.g. heparin sulfate for FMDV) (Jackson *et al.* 1996) or glycoproteins (e.g. CD155 for poliovirus) (Mendelsohn *et al.* 1989). The protein-based receptors used by picornaviruses mostly belong to the immunoglobulin superfamily (Greve *et al.* 1989, Mendelsohn *et al.* 1989, Bergelson *et al.* 1997) or integrin superfamily (Roivainen *et al.* 1994, Jackson *et al.* 2000, Williams *et al.* 2004, Xing *et al.* 2004). Some examples of proteinaceous receptors used by picornaviruses are αvβ3 integrin, αvβ6 integrin, intercellular attachment molecule-1 (ICAM-1), polio virus receptor (CD155/Pvr), decay accelerating factor (DAF) and coxsackie adeno receptor (CAR) (Greve *et al.* 1989, Mendelsohn *et al.* 1989, Shafren *et al.* 1995, Bergelson *et al.* 1997, Seitsonen *et al.* 2010). These receptors can merely act as an attachment site for the virus (Shafren *et al.* 1997, Karnauchow *et al.* 1998) or they can cause instability in the virus capsid and initiate capsid uncoating (He *et al.* 2000, Ohka *et al.* 2004).

The canyon on the capsid surface (see section 1.1.1 and Figure 1) is widely used as the site for capsid binding to cellular receptors (Olson *et al.* 1993, Kolatkar *et al.* 1999, Belnap *et al.* 2000a, He *et al.* 2000, He *et al.* 2001, Xiao *et al.* 2001) but it is not the only site, as both sides of the canyon rim and the five-fold vertices are also exploited by picornaviruses to bind to cellular receptors (Hewat *et al.* 2000, Rossmann *et al.* 2002).

The same virus can have different receptor binding sites on its capsid surface for infecting different cell types as in the case of Coxsackevirus A9 where it uses the 'arginine-glycine-aspartic acid' (RGD) motif on the capsid surface in order to gain entry into many integrin-bearing cell types like African green monkey kidney cells (Roivainen *et al.* 1991), but it can still infect human rhabdomyosarcoma cells after deletion of the 'RGD' motif, indicating the use of a second receptor-binding site (Hughes *et al.* 1995). The virus can also use different receptors on the same cell at different stages of its entry as in the case of coxsackievirus B3 (CVB3) and coxsackievirus A21 (CVA21) where they uses DAF as a binding receptor but for uncoating they require CAR and ICAM1, respectively (Shafren *et al.* 1997, Milstone *et al.* 2005).

1.1.3 Entry and RNA release

From the structural perspective, the virus must have a dynamic but stable capsid so that while escaping the harsh conditions that the virus encounters upon first contact with the human body, it can still interact with its target cell and release the RNA in the host cell cytoplasm. Picornavirus capsids can "breathe", leading to transient expulsion of the VP1 N-terminus and VP4 at a physiological temperature (Li *et al.* 1994, Lewis *et al.* 1998, Katpally *et al.* 2009, Lin *et al.* 2012). Subsequently, it has been suggested that once a cellular

receptor comes in contact with a picornavirus, it displaces the pocket factor from the β-barrel of VP1, thereby, destabilizing the virus, at least in the case of entero- and rhino-viruses which have a pocket factor. This results in capsid expansion and embedding of externalized VP1 and VP4 into the host membrane to make a channel into the cell interior so that the RNA gets released into the cytoplasm (Fricks and Hogle 1990, Danthi *et al.* 2003, Tuthill *et al.* 2006, Davis *et al.* 2008).

Although the molecular events associated with RNA release are well described in the literature, there has been controversy in the field about the exit site for RNA on the capsid. Early reports suggested the capsid vertices as the site for RNA release based on the fact that there is a plugged channel present on the five-fold vertices in virion which gets opened by externalization of VP1 N-terminus and VP4 (Hadfield *et al.* 1997, Belnap *et al.* 2000b, Belnap *et al.* 2000a, Hewat *et al.* 2002, Hewat and Blaas 2004, Bubeck *et al.* 2005b, Bubeck *et al.* 2005a). Recently, work on poliovirus has challenged the earlier RNA exit model by identifying holes near the two-fold and quasi three-fold axes in icosahedral reconstructions of early and late empty capsids suspected to be RNA exit sites (Levy *et al.* 2010) and later confirmed to be near the two-fold symmetry axis by asymmetric reconstructions where the virus was imaged at the stage of RNA release (Bostina *et al.* 2011). Owing to the low resolution of these asymmetric reconstructions from single particle work and subtomogram averaging and the fact that these particles were not true derivatives of virion-cellular interactions but were prepared by heating the virions at 56°C (Bostina *et al.* 2011), these experiments gave only indicative evidence of the RNA release site on the capsid surface. Finding the general applicability of this model to other picornaviruses was one of the motivations for the current study.

Even if the RNA comes out of a two-fold, how one site is chosen out of the 30 possible sites on the capsid and how an RNA exit site facing the cellular membrane is chosen remain unanswered questions.

1.1.4 Genome organization

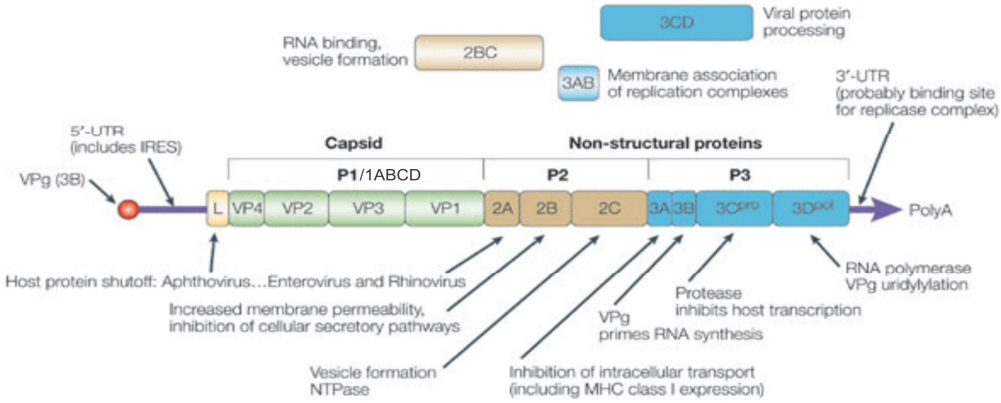

Figure 2. Poliovirus genome organization, post-translational processing and protein function.

Reprinted from Whitton J.L. *et al* Nature Reviews Microbiology 2005 with permission from Nature Publishing Group.

The picornaviruses have positive-sense, single-stranded, non-segmented RNA genomes capable of infection on its own without additional accessory proteins (Colter *et al.* 1957, Alexander *et al.* 1958, Brown *et al.* 1958). The genome can be divided into the 5' untranslated region (UTR), the coding region and the 3' UTR (Figure 2) (Kitamura *et al.* 1981). The long 5' UTR contains the viral-encoded viral protein genome-linked protein (VPg) covalently linked at its 5' end (Pettersson *et al.* 1978) and an internal ribosome entry site (IRES) (Jang *et al.* 1988, Pelletier *et al.* 1988) (Figure 2). The VPg

acts as a primer for the viral-encoded, RNA-dependent, RNA polymerase (Nomoto *et al.* 1977, Paul *et al.* 1998) and the IRES is required for RNA translation (Jang *et al.* 1988, Pelletier *et al.* 1988). Since the picornavirus RNA does not carry any accessory protein with it except VPg, the first viral action after release of the RNA in the host cell is viral RNA translation (Semler 2002).The coding region is translated as a single polyprotein which is cleaved into P1, P2 and P3 proteins by viral-encoded proteases (Figure 2) (Holland and Kiehn 1968, Jacobson and Baltimore 1968, Summers and Maizel 1968, Rueckert and Wimmer 1984). Further proteolysis cleaves P3 into 3AB and the 3CD protease. 3CD cleaves P1 into 1ABC and 1D/VP1, and P2 into 2A and 2BC (Figure 2) (Semler 2002, Bedard and Semler 2004). Viral proteins formed at this stage either start functioning for instance by shutting off the host transcription-translation machinery or undergo further cleavage whereby 1ABC cleaves into VP0 and VP3, 2BC cleaves into 2B and 2C, 3AB cleaves to form 3A and 3B, and 3CD cleaves to form 3C and 3D (Figure 2) (Semler 2002, Bedard and Semler 2004). The 3D protein is the RNA-dependent RNA polymerase and once it is made, it starts synthesizing negative-sense RNA which is later used as the template for making more of the positive-sense RNA, thereby, increasing the concentration of the viral RNA and proteins in the host cell (Semler 2002, Bedard and Semler 2004).The 3' UTR is short, with a poly-A tail at its end (Kitamura *et al.* 1981). The 3' UTR is required for the synthesis of negative-sense RNA strand from the positive RNA strand (Pilipenko *et al.* 1996).

1.1.5 Viral assembly

The double stranded, deoxyribonucleic acid (DNA) viruses (e.g. phi29 bacteriophage) or double stranded RNA viruses (e.g.phi6 bacteriophage) use

packaging motor proteins to package the viral genome into a preassembled procapsid (Gottlieb *et al.* 1991, Gottlieb *et al.* 1992, Paatero *et al.* 1998, Smith *et al.* 2001). The specificity for packaging the viral genome in these viruses comes from specific sequences on the viral genome as in the case of phi6 where these so called 'pac sequences' present on the 5'end, fold into secondary structures (Pirttimaa and Bamford 2000) and are recognized by the viral protein P1 (Qiao *et al.* 2003). Interestingly, phi6 packages its genome in the form of 3 segmented single-stranded RNAs sequentially by the help of the P4 packaging motor protein (Qiao *et al.* 1995, Paatero *et al.* 1998, Mindich 2004). The single-stranded non-segmented RNA viruses like picornaviruses lack a packaging motor protein, therefore assembly of capsid and packaging of the genome should occur simultaneously (Hohn 1976).

Picornavirus assembly is poorly understood at least at the structural level. The capsid proteins are known to assemble into pentamers which either by direct interaction with RNA form genome-filled capsids (Nugent and Kirkegaard 1995) or make empty capsids (Putnak and Phillips 1981, Corrias *et al.* 1987, Ansardi *et al.* 1991, Jore *et al.* 1991). It is still unclear whether the naturally-occurring empty capsids formed are on-pathway intermediates for RNA encapsidation (Basavappa *et al.* 1994, Curry *et al.* 1997) or dead-end products which are infection incompetent (Marongiu *et al.* 1981). In addition, which assembly intermediate is associated with RNA packaging is unclear. Only one study in a cell free system on poliovirus has directly demonstrated that it is the pentamer which is likely to be associated with packaging (Verlinden *et al.* 2000). This observation is further validated by *in vitro* assembly work on bovine enterovirus where it has been demonstrated that the dissociation of *in vitro* formed empty capsids is an energetically unfavorable

process, therefore, they are not likely to be the packing unit for assembly (Li *et al.* 2012).

The picornavirus capsid encapsidates only its own viral genome *in vivo* but where that specificity comes from is debatable. Nevertheless, it has been argued that the specificity for packaging viral RNA into the capsid comes from the viral proteins of the RNA replication complex and the viral RNA itself does not play any role in packaging or assembly (Nugent *et al.* 1999, Liu *et al.* 2010b). This argument comes from experiments where successful and efficient encapsidation of chimeric genome was observed when the poliovirus 5' UTR regions were replaced with regions from other picornaviruses such as coxsackievirus B3 (Johnson and Semler 1988) and human rhinovirus 2 (HRV2) (Gromeier *et al.* 1996, Plevka *et al.* 2012) and even with a flavivirus, hepatitis C virus (Lu and Wimmer 1996). These observations were further supported when similar experiments were conducted by removing or replacing P1, 3' UTR, P2 or VPg encoding regions of poliovirus with other viruses (Reuer *et al.* 1990, Porter *et al.* 1995, Porter *et al.* 1998). In contrast, there have been a few studies which indirectly gave evidence that there could be regions on the viral RNA genome called packaging signals (PSs) which make contact with capsid proteins and ensure that the viral genome gets packaged and not the cellular RNA (Barclay *et al.* 1998, Jia *et al.* 1998, Johansen and Morrow 2000b, a). These studies monitored the trans-encapsidation efficiency, in co-transfection of a poliovirus replicon carrying sub-genomic regions like 5' UTR regions, IRES elements or 3' UTR regions for poliovirus with the capsid proteins from poliovirus or other picornaviruses expressed on other vector (Barclay *et al.* 1998, Jia *et al.* 1998, Johansen and Morrow 2000b, a). These studies observed that the trans-encapsidation efficiency of polioviral sub-genomic regions was

significantly lower for capsid protein of other picornaviruses as compared to poliovirus. The most convincing evidence of PSs in picornaviruses perhaps comes from Aichi virus where mutations in 5' UTR stem-loop region A keep the Aichi virus mutant replication and translation efficient but instead of genome-filled virions, empty capsids were formed (Sasaki and Taniguchi 2003).

For other single stranded non-segmented RNA viruses like bacteriophage MS2 (MS2) and the plant virus, Satellite Tobacco Necrosis Virus (STNV), it has been demonstrated that specific stem-loops on the viral RNA act as PSs for the assembly of the capsid into an infectious virion (Stockley *et al.* 2007, Toropova *et al.* 2008, Basnak *et al.* 2010, Bunka *et al.* 2011, Dykeman *et al.* 2011). In fact, PSs have been identified for other RNA viruses as well such as tobacco mosaic virus (Butler and Klug 1971, Zimmern and Butler 1977), turnip crinkle virus (Qu and Morris 1997), brome mosaic virus (Choi and Rao 2003), human immunodeficiency virus 1 with the well-studied packaging signal ψ (Lever *et al.* 1989), mouse hepatitis virus (Abrescia *et al.* 2004), severe acute respiratory syndrome coronavirus (Hsieh *et al.* 2005), transmissible gastroenteritis coronavirus (Morales *et al.* 2013), rift valley fever virus (Morales *et al.* 2013) and alphaviruses (Jäälinoja *et al.* 2008). However, the most comprehensive evidence for RNA-centric assembly in icosahedrally-symmetric viruses comes from MS2.

The crystal structure of the MS2 capsid showed 30 copies of symmetrical capsid protein dimers (C/C) and 60 copies of asymmetrical capsid protein dimers (A/B) arranged in a T=3 capsid (Valegard *et al.* 1990, Golmohammadi *et al.* 1993). The capsid protein dimers were shown to initiate assembly by binding to a 19 nucleotide long RNA stem-loop structure called

the translation repressor (TR) which occurs only once in the whole genome sequence (Beckett and Uhlenbeck 1988, Beckett *et al.* 1988). The co-crystallization of capsid protein dimers not only with TR stem-loop but also with other sequences showed the plausibility of non-TR PSs for MS2 (Valegard *et al.* 1994, Valegard *et al.* 1997, Convery *et al.* 1998, Rowsell *et al.* 1998, van den Worm *et al.* 1998, Horn *et al.* 2004). Later on, several studies showed the conformational switching of the symmetric C/C dimer form to the asymmetric dimer A/B upon its binding to TR stem-loop during assembly and that the assembly requires both dimer types (Stockley *et al.* 2007, Basnak *et al.* 2010, Dykeman *et al.* 2010, Morton *et al.* 2010). Electron cryo-microscopy (Cryo-EM) in conjunction with icosahedral averaging showed 2 distinct layers of RNA density inside the wild type MS2 capsid in contact with each other (Toropova *et al.* 2008). Subsequently, a C5 symmetric reconstruction revealed a distinct density below the vertex attributed to a single copy of the maturation protein in complex with RNA termini (Toropova *et al.* 2011). This observation was later invalidated by symmetry-free subtomogram averaging of the MS2 capsid in complex with its receptor F-pilus showing the point of asymmetry at the two-fold symmetry axis occupied by a single copy of the maturation protein (MP) by restricting the angular search range on the basis of the direction and polarity of the F-pilus (Dent *et al.* 2013). The MP is responsible for two distinct roles: first is the circularization of the 5' and 3' ends of the viral RNA (Nathans *et al.* 1966, Shiba and Suzuki 1981) which require it to be inside the capsid; and second is the recognition and attachment of the F-pilus to the bacteriophage (Roberts and Steitz 1967, Krahn *et al.* 1972) which require the MP to be exposed on the capsid surface. Therefore, the presence of MP on the capsid surface partially exposed and partially in contact with the viral genome

as identified by the subtomogram-based asymmetric reconstruction gives credibility to its dual role at the structural level.

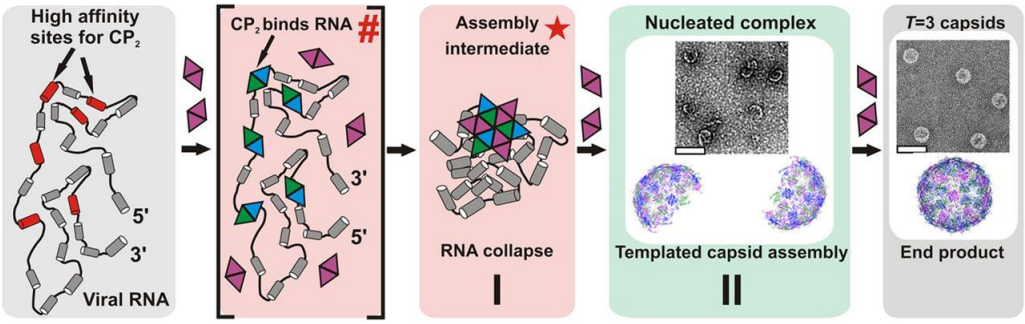

Figure 3. Two-stage model for MS2 assembly.

Reprinted with permission from Borodovka A. *et al* PNAS. Copyright (2012) National Academy of Sciences.

Recently, reassembly assays for MS2 and STNV, monitored by single molecule fluorescence correlation spectroscopy (smFCS), provided a mechanistic model for capsid-RNA coassembly (Figure 3) (Borodavka *et al.* 2012). The smFCS assays were carried out by fluorophore tagging of either the capsid proteins or the RNA to monitor capsid assembly or RNA folding, respectively. The main feature of smFCS is that these studies can be carried out at a very low concentration (<1μM) of the components under investigation mimicking the expected scenario in the physiological state (Borodavka *et al.* 2012). MS2 and STNV assembly were shown to occur in two stages. In the first stage, capsid proteins in sub-stoichiometric concentrations bound to sequence- and structure-specific regions on free-form viral RNA resulting in a quick viral RNA collapse instead of the slow compaction expected if the capsid-RNA interactions were merely electrostatic (Borodavka *et al.* 2012). This was followed by a rate-limiting second stage, where recruitment of more

capsid proteins either individually or as decamers and hexamers onto the collapsed RNA resulted in the gradual assembly of the whole capsid (Borodavka *et al.* 2012). Although assembly in the presence of equally-long, non-viral RNAs was also shown to be initiated, it was far more inefficient and no RNA collapse was seen (Borodavka *et al.* 2012). So, capsid-RNA co-assembly is a function of protein-protein and protein-RNA interactions where capsid proteins bind to PSs distributed throughout the viral RNA genome instead of a single high affinity PS. In fact, multiple PSs have been predicted for MS2 and bacteriophage GA using Hamiltonian paths (see below for description of Hamiltonian paths) (Dykeman *et al.* 2013) and for STNV using systematic evolution of ligands by exponential enrichment (SELEX) (see section 4.2 for a description of SELEX) (Bunka *et al.* 2011).

These observations about the capsid assembly pathway using multiple packaging signals along with the distribution of the RNA in the first asymmetric reconstruction of MS2 (Toropova *et al.* 2011) were described mathematically using Hamiltonian paths (Dykeman *et al.* 2011). In graph theory, a Hamiltonian path describes the route taken from one graph vertex to another using each vertex only once. Hamiltonian path descriptions for MS2 assembly were established by making assumptions on the binding of MP to the 5'- and 3'-ends of the RNA to circularize the genome and that capsid assembly follows an energetically-favored pathway. Without the constraints there were about 40,500 ways in which RNA could have been packaged in the capsid but with the knowledge from the C5 reconstruction of MS2 (Toropova *et al.* 2011) about the binding of both end of the RNA to a single copy of maturation protein beneath the vertex, reduced the number of probable hamiltonian paths dramatically to 66. These Hamiltonian pathways also emphasized the spacing

of the stem-loops on the genome to fit within the capsid. Combining the Hamiltonian paths with biochemical and structural studies can potentially be extended to other ssRNA viruses to identify packaging signals on viral genomes as has been shown for MS2 and GA bacteriophage and to describe viral assembly in general (Dykeman *et al.* 2013).

The above mentioned approaches of identifying assembly and packaging responsible protein epitopes and RNA motifs could be utilized for those picornaviruses which have partially or completely ordered viral RNA as in the atomic models of CVA9 (see section 1.3.2) (Hendry *et al.* 1999), CVB3 (Muckelbauer *et al.* 1995), coxsackievirus A6 (CVA6) (Filman *et al.* 1989), human rhinovirus 14 (Arnold and Rossmann 1990), human rhinovirus 16 (Hadfield *et al.* 1997), CVA21 (Xiao *et al.* 2005) in the HPeV1 cryo-EM density map (see section 1.3.3). However, knowledge of the capsid atomic model e.g. from X-ray crystallography and the RNA distribution from cryo-EM is a prerequisite for applying the Hamiltonian paths-based approach.

1.2. Electron cryo-microscopy

Biological science is about studying how things work within and around the whole organism and at the cellular and molecular level. It is well known that the function of a molecule is related to its structure, so it is imperative to understand molecular structure in detail. Over the years, the major workhorse for structure determination has been X-ray crystallography, the method that has contributed about 85000 out of 96000 deposited structures in the Protein Data Bank (http://www.rcsb.org/pdb/statistics/contentGrowthChart.do?content=explMethod-xray&seqid=100, accessed on 15.11.2013). Recently, nuclear magnetic

resonance (NMR) spectroscopy and cryo-EM are also making in-roads at similar (Bjorndahl *et al.* 2007) or lower resolution (Seitsonen *et al.* 2010). X-ray crystallography can be used to solve structures for homogenous samples ranging from small molecules (Mu *et al.* 2013) to viruses (MDa) (Abrescia *et al.* 2004, Cockburn *et al.* 2004) with the prerequisite that diffracting crystals form for which the phases can be solved. NMR spectroscopy based structure determination is mostly employed for smaller-sized homogenous proteins in a hydrated solution state and is useful especially for proteins which have flexible/unstructured regions (Felli and Pierattelli 2012). Big macromolecular assemblies like viruses or metastable ribosome complexes which are not amenable to crystallization and too big for NMR can be studied using cryo-EM in a near native state (Fischer *et al.* 2010, Zhang *et al.* 2013). The samples do not necessarily have to be homogenous for cryo-EM as they can be purified digitally from the micrographs (Fischer *et al.* 2010, Ramrath *et al.* 2012). Other information which can be pulled out using cryo-EM is different conformational states of a macromolecule or an assembly (Fischer *et al.* 2010, Ramrath *et al.* 2012). The majority of my thesis work utilizes cryo-EM (study I, II, III and IV), so I will give a brief introduction to the technique in the following sections.

1.2.1 Transmission electron microscope

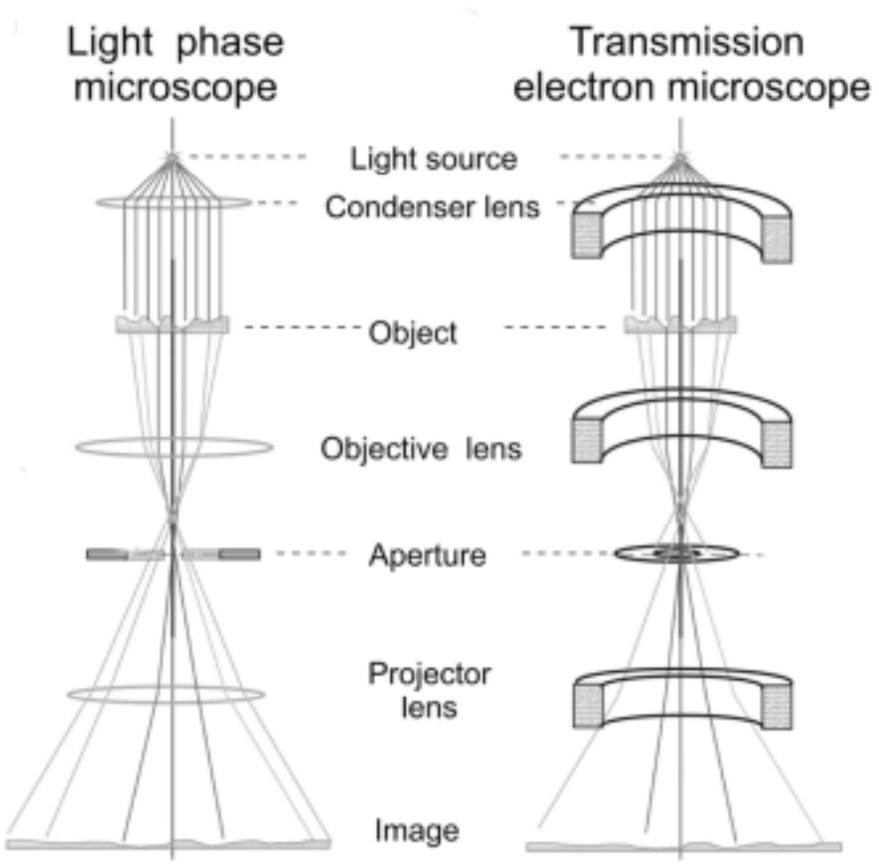

Figure 4. Comparison of light and transmission electron microscopes.

Adapted with permission from Orlova E. *et al* Chemical Reviews. Copyright (2011) American Chemical Society.

A transmission electron microscope (TEM) is analogous to an inverted light compound microscope (Figure 4) and is composed of an electron emission source, an electromagnetic lens system, objective and condenser apertures and image detection systems like a phosphor viewing screen, photographic film or

CCD camera (Orlova and Saibil 2011). The microscope is maintained at high vacuum to avoid interaction of high energy electrons with anything except the sample (Orlova and Saibil 2011). The sample is inserted into the microscope either using a side entry holder or a top entry holder. The electrons are extracted from a heated emission source which could be a tungsten filament, lanthanum hexaboride crystal, tungsten crystal based field emission gun (Orlova and Saibil 2011). The magnification and focusing of electron beams is controlled by a series of magnetic lenses, comprising condenser, objective and projection lenses (Orlova and Saibil 2011). These lenses are imperfect in shape and suffer from spherical aberrations. The spherical aberration is constant for a particular microscope and can be corrected during image processing. Actually, it is this aberration which is one of the factors that give contrast to unstained vitrified samples imaged in a TEM (Baker *et al.* 1999). The electrons can pass through the specimen without any interaction (unscattered) or on interaction with the specimen can be either elastically scattered where the travelling electrons do not loose energy or inelastically scattered where the travelling electrons loose energy (Baker *et al.* 1999, Orlova and Saibil 2011). The interaction of the electrons with the specimen gives rise to amplitude/scattering contrast and phase/interference contrast. If we consider the wave nature of the electron, then the amplitude contrast arises from the difference in the amplitude of two travelling elastic and inelastic scattering waves and is a major source of contrast for thick or stained samples. The phase contrast comes from the phase difference between elastically scattered and unscattered waves and is a major source of contrast in thin unstained samples (Baker *et al.* 1999, Orlova and Saibil 2011). Phase contrast can be enhanced by underfocussing the image which changes the path lengths of the scattered electrons more compared to the unscattered electrons without a significant loss in resolution because of the

large depth of focus of the magnetic lenses compared to the specimen thickness (Orlova and Saibil 2011).

1.2.2 Sample preparation and imaging

Biological samples, especially proteins, made of low atomic weight elements do not scattered electrons appreciably. With the aid of heavy metals stains such as uranyl acetate or tungstate high amplitude contrast can be gained but the samples may suffer from dehydration which can give rise to artifacts due to collapse of the structure and are mainly useful for low resolution work. After pioneering work on the vitrification of water (Dubochet 1981), it has been possible to image samples in a near native state by rapidly cooling the samples in liquid ethane kept in a bath of liquid nitrogen so that the samples become suspended in a glass-like state (vitrified) of water. This metastable state can be maintained in the vacuum of the microscope by keeping the temperature below ~ -160°C so as to prevent conversion of vitrified water into crystalline ice which occurs at temperatures of ~ -140°C (Baker *et al.* 1999). Cooling of samples also helps prevent radiation damage but the unstained samples inherently suffer from low phase contrast (Taylor and Glaeser 1976). So, in order to increase the ratio of signal to noise, many particles from the images are averaged together.

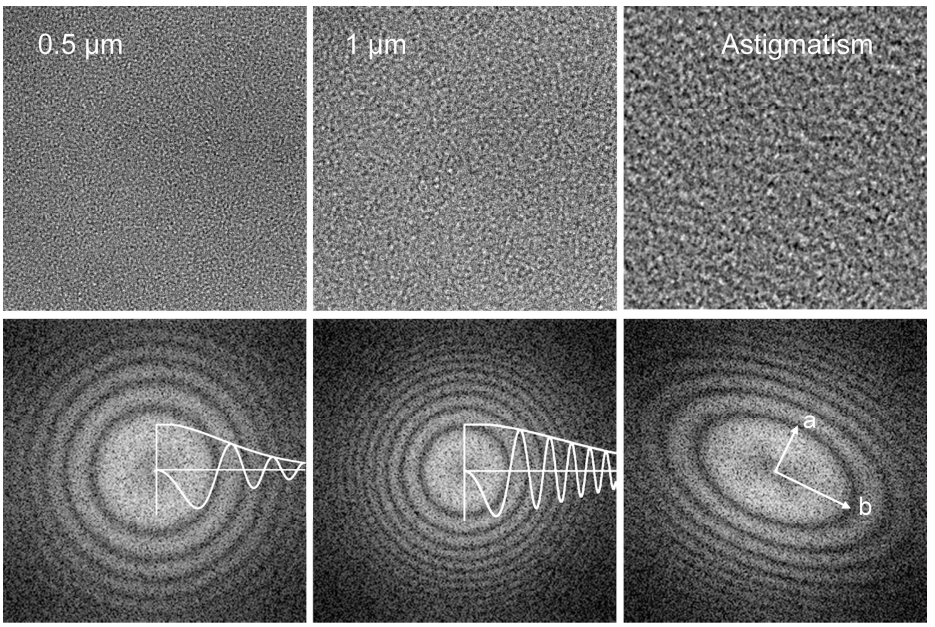

Figure 5. Thon rings and contrast transfer function.

Reprinted with permission from Orlova E. *et al* Chemical Reviews. Copyright (2011) American Chemical Society.

It is important to remember that images formed in the transmission electron microscope are projections of their three-dimensional (3-D) objects (Orlova and Saibil 2011). The relationship between the projection image and the sample itself is defined by the contrast transfer function (CTF) (Baker *et al.* 1999). The contrast transfer function (CTF) comprises of amplitude and phase scattering components and is given by the following equation:

$$CTF(v) = -\left[\left(1 - F_{amp}^2\right)^{1/2} * \sin \chi(v) + F_{amp} * \cos \chi(v)\right] * E(v) \qquad \text{-Equation (1)}$$

$$\text{where } \chi(v) = \pi * \lambda * v^2 \left(\Delta f - 0.5 * C_s * \lambda^2 * v^2\right) \qquad \text{-Equation (2)}$$

is the phase shift function with Δf as the defocus value (μm), $\sin\chi(v)$ is the phase contrast, $\cos\chi(v)$ is the amplitude contrast, F_{amp} is the fractional amplitude contrast, λ is the electron wavelength (Å) and v is the spatial frequency ($Å^{-1}$) and C_s is the spherical aberration (mm) of the objective lens (Baker *et al.* 1999). $E(v)$ is the envelope function given by

$$E(v) = e^{-(\delta v)^2} \qquad \text{-Equation (3)}$$

and dependent on beam coherence and specimen drift. The F_{amp} for an unstained cryo-EM sample is close to 0.07 (Toyoshima and Unwin 1988) which makes the phase contrast the dominant component in the CTF (Equation 1). The phase scattering itself depends on the amount of underfocus, the spherical aberration of the objective lens and the electron wavelength (Equation 1 and 2). Due to the spherical aberration in lenses, we see black and white rings called Thon rings appearing in a Fourier transform of the projection image when images are taken underfocus (Figure 5) (Baker *et al.* 1999). The rings indicate that the image details alternate among black features (negative), featureless (no information or zero) and white features (positive) at different spatial frequencies, this is called phase inversion (Baker *et al.* 1999). So, this means that some details cannot be resolved as we do not have the information at that spatial frequency; therefore, we need to record images at different underfocii to get a 3-D reconstruction. In addition, many such phase inversions are needed to be corrected in order to get to high resolution.

Imaging under cryo conditions is done at a low electron dose typically ~5-20 electrons/$Å^2$ so as not to damage the unstained hydrated sample which is extremely sensitive to radiation damage (Baker *et al.* 1999). The images are

recorded on photographic film or charged coupled device (CCD) (Faruqi and Henderson 2007) and more recently on direct electron detectors (DED) (McMullan *et al.* 2009). The images are recorded on films by interaction of electrons with silver halide crystals present in photographic emulsion, these electron-exposed films are later on dipped into developer solution followed by fixer solution so that silver halide crystals transform into visible silver grains (Orlova and Saibil 2011). Film is the recording medium of choice for the collection of high resolution data owing to the high dynamic quantum efficiency (DQE) which is a function of contrast and resolution, larger imaging area and finer pixel size (Grigorieff and Harrison 2011). There are several examples where film has been used to record data resulting in high resolution structures of icosahedral viruses including rotavirus double-layered particle (Zhang *et al.* 2008b), rotavirus VP7 recoated particle (Chen *et al.* 2009), rotavirus triple-layered particle (Settembre *et al.* 2011), bovine papillomavirus (Wolf *et al.* 2010), aquareovirus infectious sub-virion particle (Zhang *et al.* 2010), adenovirus (Liu *et al.* 2010a) and dengue virus (Zhang *et al.* 2013). Images on CCD are recorded by converting the electrons into photons using a scintillator which passes the photons to photosensitive elements of the CCD chip to convert them into an electric signal (Downing 1995). The advantage of using CCD is that a digitized image is immediately available for image processing compared to photographic films which need to be developed and digitized first. However, in comparison to film, CCD has a lower DQE at higher spatial frequencies, larger pixel size and smaller imaging area. Recent advances in DED technology, start to make them a real alternative to films and they are already far superior to CCD at 300 kV (Campbell *et al.* 2012). The image is recorded in DED by direct exposure of pixel detectors to the incident electrons (Faruqi and Henderson 2007). These pixel detectors are coupled to a

complementary metal oxide semiconductor (CMOS) to convert the signal into voltage which makes the image recording faster. Two main advantages of DED have been reported, firstly, beam-induced specimen drift and beam damage can both be minimized by careful processing of the image series acquired of each region, and secondly, the DQE is similar or may be even higher than that of photographic film, depending on the operating voltage (Campbell *et al.* 2012). This helps to increase the signal to noise ratio and contrast in the images which has resulted in more accurate determination of orientations and origins improving resolution(Campbell *et al.* 2012). Already, DED data have been processed to high resolution reconstructions for various macromolecular assemblies such as rotavirus (Campbell *et al.* 2012), eukaryotic ribosome (Bai *et al.* 2013), proteasome (Li *et al.* 2013), *Sulfolobulus* turreted icosahedral virus (Veesler *et al.* 2013) and mammalian transient receptor potential channel 1 (Liao *et al.* 2013).

1.2.3 Three dimensional image reconstruction

To combat the low signal-to-noise ratio in low dose cryo-EM images of viruses many different images can be averaged together. The viruses tend to be randomly oriented in the vitreous water, so each micrograph can contain many different views of the same virus if that virus is structurally congruent. Thus the spatial orientations and position of the images with respect to each other or to a reference image (Baker *et al.* 1999) need to be determined. Inherent symmetry present within the specimen can be used to improve the resolution of the map (Baker *et al.* 1999).

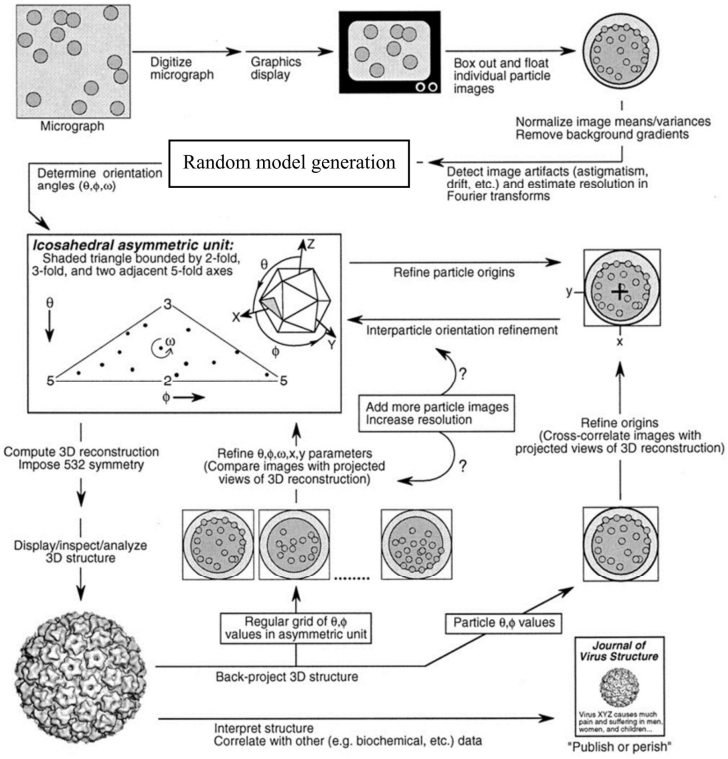

Figure 6. General workflow of image processing.

Modified with permission from Baker T.S. *et al* Microbiology Molecular Biology Reviews. Copyright (1999) American Society for Microbiology.

A general workflow for 3-D icosahedral image reconstruction is shown in Figure 6. The CTF (see section 1.2.2) is determined for each micrograph and the micrographs showing drift or astigmatism are discarded. There are many programs for determining the CTF of a micrograph, one such popular program is CTFFIND3 (Mindell and Grigorieff 2003) where the defocus and astigmatism determination for a micrograph is fully automated and the power spectrum of the micrograph is fitted to a calculated one. The virus particles are boxed out from the selected micrographs and are normalized to have similar

grey scale. The main goal of image reconstruction is to determine as accurately as possible spatial orientations and origin values for the boxed virus particles. The particle orientations is commonly determined by the common lines method (Crowther 1971) or projection matching (Baker and Cheng 1996, Fuller *et al.* 1996) for icosahedral viruses distributed randomly in vitrified ice. The common line approach works on the principle that in Fourier space different two-dimensional projections of a 3-D object have at least one common line (De Rosier and Klug 1968). Therefore relative orientation between different particles can be determined in Fourier space from three or more common lines between them. For high symmetry objects the number of these common lines is rather high as in the case of an icosahedron where 6 five-fold axes contribute 12 common lines, 10 three-fold axes contribute 10 common lines and 15 two-fold axes contribute 15 common lines which together have 37 pairs of common line per particle and 60 pairs of cross-common lines between two particles (Crowther 1971). Instead of Fourier space, the common line method can be alternatively applied in real space using angular reconstitution (Van Heel 1987).

An initial model is a prerequisite in projection matching approach. The initial model can be a known related 3-D structure, an object of similar shape and size (Baker and Cheng 1996, Fuller *et al.* 1996), a starting model from tomography (Sperling *et al.* 1997), or a series of random models generated from the boxed particles (Yan *et al.* 2007). The initial model is back projected in Fourier space in all possible orientations with predefined angular sampling and compared to 2-D projections of the boxed particles. The highest correlating projections are taken as the orientations of the boxed particles. These orientations are further refined with finer angular sampling.

In case of random model generation, a subset of particles are assigned random orientations with the assumption that the virus particle center is same as the center of the box in which it is extracted. A 3-D model is calculated and the orientations are further refined by projection matching the boxed particles against the initial model (Yan *et al.* 2007). The results from a number of such random models are compared, typically 10, and the one with the highest resolution is picked to be used as a model to determine the orientations of the full data set. The advantage of this approach is that it avoids model bias in the initial stages of the reconstruction. Irrespective of the choice of the initial model, the further refinements of orientation and origin require iterative processing where the model reconstructed in the last iteration is used as a reference model for determination of orientation and origins in the next iteration.

Many icosahedrally-symmetric virus capsids have components that do not follow that symmetry but have one or many asymmetric features in them e.g. tailed bacteriophages (Parent *et al.* 2012), sub-stoichometrically saturated soluble receptors on icosahedral viruses (Hafenstein *et al.* 2007, Seitsonen *et al.* 2010), genome density in an icosahedral capsid (Toropova *et al.* 2011, Dent *et al.* 2013), single-copy protein in the capsid (Dent *et al.* 2013), mismatches in symmetry of the capsid proteins (Briggs *et al.* 2005, Huiskonen *et al.* 2007, Jäälinoja *et al.* 2008). Imposing icosahedral symmetry during 3-D reconstruction averages out such features. There are different approaches to obtain an asymmetric reconstruction (Tao *et al.* 1998, Morais *et al.* 2001, Briggs *et al.* 2005, Lander *et al.* 2006, Hafenstein *et al.* 2007, Bostina *et al.* 2011, Toropova *et al.* 2011, Parent *et al.* 2012), one such approach is to mask the asymmetric parts initially and impose icosahedral symmetry until optimal

origins and orientations of the virus particles are determined (Tao *et al.* 1998, Morais *et al.* 2001, Lander *et al.* 2006, Parent *et al.* 2012). Next, the icosahedral symmetry can be relaxed and the asymmetric features are unmasked from the virus particles. A new set of orientations are determined for these particles by aligning the asymmetric features in each particle to a common reference which have a single copy of the asymmetric feature at a predefined position in its structure (Tao *et al.* 1998, Morais *et al.* 2001, Lander *et al.* 2006, Parent *et al.* 2012).

The information from these 3-D density maps can be extended by fitting atomic models into its 3-D density map in order to obtain 'pseudo-atomic models (Stewart *et al.* 1991, Olson *et al.* 1993, Grimes *et al.* 1997, San Martin *et al.* 2001, Zhang *et al.* 2008a, Shingler *et al.* 2013). These atomic models for the whole virus, its individual components or structural homologs are derived from X-ray crystallography, NMR (Fabiola and Chapman 2005, Rossmann *et al.* 2005) or *in silico* homology modelling (Topf and Sali 2005, Roy *et al.* 2010) and are fitted either by rigid or flexible fitting (Topf *et al.* 2008, Ahmed *et al.* 2012, Lopez-Blanco and Chacon 2013). Even for rigid fitting, the resolution of the reconstruction, the completeness of the atomic model, the predominant secondary structure elements and the shape of both the atomic model and the reconstruction are key factors when trying to find the best fitting solutions. But in addition, the atomic models and the 3-D density maps may have conformational differences which could be due to flexible loop regions of the structure or major changes in the conformation states of the atomic model and the density map or there could be protein structure prediction errors arising from homology modelling (Topf *et al.* 2008, Ahmed *et al.* 2012). In order to do fitting for such cases, perturbation of the atomic model is required to find the

optimal conformation of the model with respect to the 3-D density map in conjunction with search for best fits of origins and orientations (Topf *et al.* 2008, Ahmed *et al.* 2012, Lopez-Blanco and Chacon 2013). Still there is a need to generalize and test these methods especially for homology models.

1.3. Viruses in this study

1.3.1 Coxsackievirus A7

Coxsackievirus A7 (CVA7) is a member of the *Enterovirus A* (EV-A) species whose other clinically important members are enterovirus 71 (EV71) and coxsackievirus A16 (CVA 16). EV71 and CVA16 are the main causative agents for hand, foot and mouth disease (Hagiwara *et al.* 1978, Cabrerizo *et al.* 2013) whereas CVA7 is similar to poliovirus in pathogenesis (Ranzenhofer *et al.* 1958) and is associated with acute flaccid paralysis (Habel and Loomis 1957, Grist 1962) and aseptic meningitis (Richter *et al.* 1971).

Strain-based variations in pathogenesis and tropism are seen for CVA7 in EV-A group. CVA7 Parker and USSR strains are associated with flaccid paralysis (Grist 1962) whereas 275/58 strain is associated with aseptic meningitis (Richter *et al.* 1971); even the infection in animal models differ among these strains (Habel and Loomis 1957, Richter *et al.* 1971).

Earlier, unlike EV71, human scavenger receptor class B, member 2 (SCARB2) was not considered a cellular receptor for CVA7 (Yamayoshi *et al.* 2009) but a recent study showed it to be a likely receptor for CVA7 (Yamayoshi *et al.* 2012). This discrepancy was due to the successful infection of CVA7 Parker strain in SCARB2 expressing cells as well as SCARB2 deficient cells (Yamayoshi *et al.* 2009), however, SCARB2 knockdown by

RNA interference in a SCARB2 expressing cell line showed loss of CVA7 Parker strain infection which was regained in rescue experiments (Yamayoshi *et al.* 2012). So, CVA7 infection in SCARB2 expressing cells is SCARB2 dependent but it is likely to utilize other receptors in non-SCARB2 expressing cells.

Clearly, CVA7 and other members of the EV-A group are clinically a significant group of viruses but there was no structural information available on these viruses when study I was initiated.

1.3.2 Coxsackievirus A9

Coxsackievirus A9 (CVA9) is a member of the *Enterovirus B* species whose other important members are CVA6, CVB3 and echovirus 1. These viruses are associated with various diseases such as respiratory infection (Whitton *et al.* 2005), aseptic meningitis (Michos *et al.* 2007, Cui *et al.* 2010), myocarditis (Moschovi *et al.* 2007), encephalitis (Moschovi *et al.* 2007) and childhood diabetes (Clements *et al.* 1995, Roivainen *et al.* 1998). CVA9 is known to utilize integrins αvβ3 and αvβ6 for cellular entry by attaching through its VP1 C-terminus 'RGD' motif (Roivainen *et al.* 1994, Williams *et al.* 2004), although, successful infection with an 'RGD' less mutant has also been reported (Roivainen *et al.* 1996).

These integrins are essential cellular receptors which facilitate cell adhesion (Ross *et al.* 2013), cell migration (Huttenlocher and Horwitz 2011) and cell differentiation (Streuli 2009). These heterodimers of α-and β-type chains are exploited for their 'RGD' motif recognition capabilities by many viruses for cell attachment and internalization (Stewart and Nemerow 2007). Cryo-EM in combination with other techniques revealed that viruses can bind

to different conformation state integrins as shown for echovirus 1 binding to bent state integrin (Xing *et al.* 2004, Jokinen *et al.* 2010) or the adenovirus binding to an extended state integrin (Lindert *et al.* 2009). Similar to natural integrin ligands, the virus binding can induce transition in the integrin state from one conformation to another (Lindert *et al.* 2009) and also cause clustering of integrins in the cell membrane (Jokinen *et al.* 2010).

Although there is an atomic model available for CVA9 (Hendry *et al.* 1999) (PDB: 1D4M), unlike echovirus 1 (Xing *et al.* 2004, Jokinen *et al.* 2010), the structural basis for its binding to the integrins was not established prior to this study. The CVA9 atomic model possesses the common characteristics of an enterovirus such as a T=1 (pseudoT=3) capsid, the presence of a canyon, hydrophobic pocket factor and VP4 inside the capsid shell (see section 1.1.1) (Hogle *et al.* 1985, Hendry *et al.* 1999). An RNA nucleotide density in contact with a highly conserved tryptophan residue of capsid protein VP2 was also seen in this structure (Hendry *et al.* 1999). However, RNA expulsion from the capsid could not be elicited from this model.

1.3.3 Human Parechovirus 1

Human parechoviruses (HPeV) 1-16 are members of the *Parechovirus* genus, although HPeV1 and HPeV2 were originally named as echovirus 22 and 23, respectively, under the genus, *Enterovirus* (Wigand and Sabin 1961). However, the genome sequencing and N-terminal sequencing of VP1 and VP3 showed HPeV1 to be distinct from other picornaviruses (Hyypiä *et al.* 1992) and was later categorized into separate parechovirus group. HPeV1 infections usually occur in early childhood with mild respiratory (Russell and Bell 1970,

Abed and Boivin 2006) and gastrointestinal infections (Grist *et al.* 1978, Ehrnst and Eriksson 1993). However, in some cases these infections can lead to severe diseases of the central nervous system like aseptic meningitis (Ehrnst and Eriksson 1993), encephalitis (Koskiniemi *et al.* 1989) and encephalomyelitis (Legay *et al.* 2002) or myocarditis (Maller *et al.* 1967, Russell and Bell 1970).

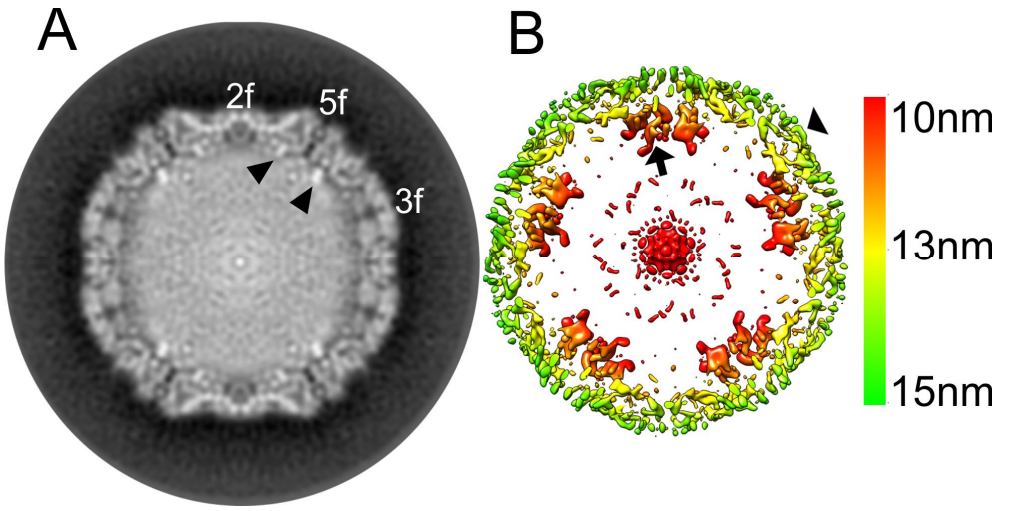

Figure 7. HPeV1 capsid-RNA finger-like densities.

A) Central cross section of HPeV1 EM density map (EMDB: 1690) (Seitsonen *et al.* 2010) with capsid-RNA densities marked with arrow-head. The view is along the two-fold axis. Two-fold, five-fold and three-fold symmetry axes are marked as 2f, 5f and 3f, respectively. B) Slabbed-section of isosurface, radially depth-cued HPeV1 EM density map (EMDB: 1690) (Seitsonen *et al.* 2010) rendered at 3 standard deviation above mean showing the capsid-RNA density marked by arrow. Arrow-head indicates the density for capsid shell. Color key based on distance from the center of the particle is shown.

Cell culture studies have shown that HPeV1 can grow in a wide variety of cell lines and is most efficient in HT29 cells (Westerhuis *et al.* 2013), indicative of broad cellular tropism with utilization of many different cellular

receptors. As in the case of CVA9 and echovirus 9, HPeV1, 2, 4, 5 and 6 also have an 'RGD' motif on the VP1 C-terminus and binding to 'RGD' recognizing integrins such as αvβ3 and αvβ6 have been shown for HPeV1 (Boonyakiat *et al.* 2001, Joki-Korpela *et al.* 2001). The structural basis for this binding was established in a cryo-EM study on integrins αvβ3 and αvβ6 with the virus (Seitsonen *et al.* 2010). A surprising observation which came out of this work was the identification of highly ordered capsid-RNA densities below the vertices with the signal intensity as high as that for the capsid proteins (Figure 7) (Seitsonen *et al.* 2010). These densities seemed unique to the parechoviruses as none of the earlier reported cryo-EM or X-ray structures for picornaviruses have reported them. We are still debating reason behind this strong RNA-capsid association.

2. AIMS OF THE STUDY

The general aims of these studies were to understand the mechanism(s) underpinning picornavirus-host cell interactions at the structural level. More specifically, we wanted to understand how picornaviruses interact with the cellular receptors; what happens to them upon RNA release; how do they assemble; where does the specificity of assembly comes from? I studied CVA7, CVA9 and HPeV1 with the following specific aims in mind:

A. CVA7: To understand this virus structure as there was no structural information available for this virus group at the beginning of the study. To understand why different strains of CVA7 differ in pathogenesis and tropism; and what happens to the capsid when RNA is released?

B. To improve methods of fitting and validation of homology models and their fits into complex structures that undergo conformational changes.

C. CVA9: To understand the virus-receptor interaction in greater detail using cryo-EM utilizing the known atomic structure of the capsid. Also, to understand the conformational changes in the capsid on RNA egress upon binding to cellular receptors.

D. HPeV1: To understand RNA-based assembly of picornaviruses using HPeV1 as a model system because this virus shows strong interactions at the interface of the capsid proteins and the viral genome.

3. MATERIALS AND METHODS

The majority of the thesis is about the determination of the virus structures either in isolation or in complex with soluble cellular receptors. Although the virus structure can be determined either by X-ray or using electron cryo-microscopy, the choice depends on the sample properties. When the sample is structurally homogenous, of reasonable size and crystallizes then X-ray is the method of choice but in this work, the samples were a mix of genome-filled and empty capsids and when they were in complex with receptors, there was variability in terms of the number of receptors bound to the capsid. So for these reasons, electron cryo-microscopy was employed. In addition, the inherent icosahedral symmetry present in these viruses was imposed in the 3-D image reconstruction which gives a reasonable virus reconstruction with a lower number of particles as described in details in 'material and method' section of study I and II (also see section 1.2.3). Besides, icosahedral reconstruction, asymmetric reconstruction was also carried out for receptor-virus complexes in study II because receptor binding to the virus was suboptimal causing its density to smear in the icosahedral reconstruction. In order to investigate the reason behind this sub-stoichometric binding of the receptor to the capsid, we adopted the asymmetric reconstruction approach used for tailed Sf6 bacteriophages (Parent *et al.* 2012). I modified this asymmetric reconstruction method by manually attaching a receptor density on one of the 60 equivalent binding positions on a capsid and using it as the reference map for aligning one of the 60 possible positions of receptor-bound virus capsid particles in the asymmetric mode of AUTO3DEM. This asymmetric method helped us to describe the steric hindrance caused by receptor binding to the virus.

The combination of icosahedral reconstruction with flexible fitting (see section 2.3) was maximally utilized in study I and II. Flexible fitting of poor homology models into sub-nanometer resolution 3-D density maps (study I) was particularly challenging in terms of segmentation of the predominantly β-sheet density map, fitting at the interfaces of the capsid proteins, fitting of flexible regions and identification of unreliable regions due to errors in the homology modelling. The lessons learnt from flexible fitting using two different approaches in study I and II led us to develop a general protocol for fitting homology models in low resolution virus 3-D density maps (study III). Study III also demonstrated methods of modelling remote homologs into density maps, modelling of expansion states of macromolecules using known X-ray structures into EM density maps. Finally, study III combined the results for homology models of two different conformational states especially looking at the validation and comparison of different approaches.

Table 1 Methods used in the study

Method	**Used in the study**
Virus culture and purification	I, II, IV
Electron cryo-microscopy	I, II, IV
Three dimensional image reconstruction	I, II
Homology modelling	I, III
Rigid and flexible fitting	I, II, III
Reverse transcription- polymerase chain reaction	I, IV
Sequence alignments	I, IV
Viral RNA extraction	I
DNA sequencing	I

Mammalian cell culture	I, II, IV
Recombinant protein purification	II
Electron cryo-tomography	II
Asymmetric reconstruction	II
Difference imaging	II
Surface plasmon resonance	II
Biotin labeling	IV
Native polyacrylamide gel electrophoresis	IV
RNA SELEX	IV
Polymerase chain reaction	IV
Next generation sequencing	IV
Thermophoresis	IV

4. RESULT AND DISCUSSION

4.1. RNA: cause and effect in viral entry

Virus capsids are metastable, undergoing a series of structural changes mainly in response to external factors such as interaction with the cellular receptors with the sole aim of multiplying the viral genome by infecting the host. In return, the genome stores all the information which the virus capsids will require for successful infection. In study I and II, we have looked at different events; all associated with a single goal of viral entry into a suitable host so as to release its RNA.

Conformational changes in capsid upon RNA release

The events occurring in the capsid on RNA release had largely been an unaddressed question in the field until recently. In study I & II, three-dimension reconstruction maps of CVA7 and CVA9 genome-filled and empty capsid were determined to between 6-10 Å, where α-helices were evident, but individual β-strands were difficult to discern. The CVA7 maps were fitted with homology models derived from I-TASSER (Roy *et al.* 2010) whereas the CVA9 atomic model (PDB: 1D4M) (Hendry *et al.* 1999) was utilized to fit into the CVA9 maps. By comparing the fitted models into the genome-filled and empty maps, the regions in the capsid undergoing conformational changes were identified. In addition, these changes in translation and rotation were quantified using a component placement score (Topf *et al.* 2008) for the corresponding capsid proteins and individual secondary structure elements between genome-filled and empty capsid fits. This had the advantage of allowing easy description of the key changes occurring, that were not evident by visual

inspection of the 3-D reconstructions alone. The largest translation observed was for VP1 in both CVA7 and CVA9 whereas most of the rotation was contributed by VP2 and VP3. The homology models of CVA7 were improved by the inclusion of the EV71 atomic models that were published in the interim (Plevka *et al.* 2012, Wang *et al.* 2012). This led to reduction in the component placement score compared to the one reported in study I and was actually more in line with concurrent results that came out for EV71 (Wang *et al.* 2012) and CVA16 (Ren *et al.* 2013). Taken together, these results for CVA7 and CVA9 indicated that the release of RNA is a concerted interplay between capsid proteins VP1-3 which resulted in expansion of the capsid, through VP2 and VP3 rotation of ~5°and VP1 translation of ~4Å. Recently, it has been shown that this results in externalization of the VP1 N-terminus and expulsion of VP4 and RNA for PV1 (Bostina *et al.* 2011), EV71 (Wang *et al.* 2012), HRV2 (Garriga *et al.* 2012) and CVA16 (Ren *et al.* 2013). Given the similarity of the conformational changes between these different viruses, it is likely that VP1 and VP4 are critical for RNA release in both CVA7 and CVA9.

Does RNA exit from two-fold holes?

The effect of these conformational changes can be readily appreciated at the two-fold axis of symmetry where the symmetry-related helices of VP2 move apart in the empty capsid as compared to the genome-filled capsid making the capsid porous in CVA7 and CVA9. These observations are in agreement with recent studies on expanded intermediate capsids of PV1 (Levy *et al.* 2010, Bostina *et al.* 2011), CVA16 (Ren *et al.* 2013), HRV2 (Pickl-Herk *et al.* 2013) or empty capsids of EV71 (Wang *et al.* 2012) and HRV2 (Garriga *et al.* 2012) where the expansion of the capsid and the rearrangement of the capsid proteins creates holes on the two-fold symmetry axis, which are

proposed to be RNA exit sites. This has been a matter of controversy in the literature, as the initial suggestions were that release happened through the vertices (Hadfield *et al.* 1997, Belnap *et al.* 2000b, Belnap *et al.* 2000a, Hewat *et al.* 2002, Hewat and Blaas 2004) (see section 1.1.3), so attempts to investigate poliovirus uncoating into liposomes assumed C5 symmetry and used a marker placed on the digitized data (Bubeck *et al.* 2005a). Just as with MS2 (Toropova *et al.* 2011, Dent *et al.* 2013), the assumption was false (see section 1.1.5). Latter attempts with tomography have given lower resolution results where the accurate pinpointing of the release has proven difficult (Levy *et al.* 2010, Bostina *et al.* 2011). The problem is exacerbated both by the featurelessness of picornavirus capsids, making orientation determination very difficult even at 10 Å resolution, and by the lack of a directional, well-structured internal control to constrain the refinement during subtomogram averaging, such as the F-pilus used in MS2(Dent *et al.* 2013) (see section 1.1.5). The recent crystal structure of an expanded intermediate CVA16 capsid where the VP1 N-terminus (residue number 62 onwards, 1-61 residues unresolved) is seen protruding out of the capsid and making the two-fold holes large enough supports the argument that the RNA comes out of the two-fold (Ren *et al.* 2013) as observed in low resolution cryo electron-tomograpms of an expanded poliovirus intermediate (Bostina *et al.* 2011). Furthermore, in recent work on HRV2 it has been demonstrated that the RNA obtains an ordered conformation prior to its release (Pickl-Herk *et al.* 2013) and the release is directional with the 3' end of the RNA egressing first from the capsid (Kumar and Blaas 2013) which could be plausible because the comparatively short 3' UTR have less secondary structure than the longer 5'UTR.

Is RNA release, a multi-step process?

In study II of this thesis, the structural changes in the CVA9 capsid on binding to its high affinity soluble receptor integrin αvβ6 (Heikkilä *et al.* 2009) were determined. From surface plasmon resonance, the Kd of the binding of integrin αvβ6 to surface coupled CVA9 was in the subnanomolar range. These integrin binding kinetics could be modelled either as two-state binding or parallel-reaction binding. The two-state binding model assumes change in integrin conformation upon binding to the virus whereas the parallel-reaction assumes that two different conformations of the integrin bind to the capsid either with different affinities or on different binding sites on the capsid. Both the kinetics models could be advantageous to virus infection. In accordance with the two-state model, the virus could bind to only one conformation of the integrin, leaving fewer potential ways for binding on cell surface, however, if the virus binding immediately cause change in integrin conformation that cascade into a series of events leading to internalization of integrin and virus entry then this two-state model could be advantageous for virus entry. Based on the parallel-reaction model, the virus could bind different conformational state integrins which increase the chance of virus binding to the cell surface; hence, this kinetic model could also be helpful in increasing the infection probability of the virus. Irrespective of the chosen kinetic models, the integrins did not occupy all sites on the capsid. This partial occupancy was observed from cryo-ET where different numbers and conformations of integrins were seen bound to the capsid surface. This variation in integrin conformation, high flexibility and low number of bound molecules on the capsid caused smearing of the integrin density on the capsid surface in the icosahedral reconstruction. To test whether or not this weaker density of integrin on capsid surface was due to steric hindrance, I made an asymmetric reconstruction of the CVA9-integrin genome-

filled capsid. To perform the asymmetric reconstruction, I prepared a reference model of integrin αIIbβ3 β-chain (PDB: 3FCS and 3FCU) (Zhu *et al.* 2008) attached to CVA9 genome-filled capsid at the position determined from CVA9-integrin αvβ6 icosahedral reconstruction. An orientation search was performed for each CVA9-integrin αvβ6 particle where one of the integrin on CVA9 surface was aligned to the reference model. This resulted in alignment of one integrin to the reference model whereas the rest of the integrins could be randomly distributed over the other 59 positions. The signal on the other 59 positions could be equal or stronger at some positions due to preferential distribution caused by either steric hindrance or cooperative binding. The asymmetric reconstruction showed strong density at the position where one of the integrin was aligned to the reference model whereas the rest of the other four equivalent positions around the same five-fold vertex showed weakest integrin signals at the positions closest to where the integrin aligned to the reference model. Using a reference model, where the integrin was bound to an incorrect position on the capsid such as the five-fold vertex showed a comparatively weaker density for the aligned integrins, in addition, density for the other 59 equivalent positions were also weaker in the incorrect model. This implied that the alignment of integrins on the other equivalent 59 positions is much more accurate when the model with integrin attached at the correct position was used. Overall, the asymmetric reconstruction showed that integrin binding to one of the five equivalent sites around the same vertex caused steric hindrance to binding of integrins on either side of it, however, the conformation of the bound integrin could not be discerned from this method.

By iMODfit based flexible fitting (Lopez-Blanco and Chacon 2013) of the CVA9 atomic model (PDB: 1D4M) (Hendry *et al.* 1999) into the capsid

with and without integrin and performing superimposition of the fits on each other showed no integrin-induced structural changes in the capsid proteins. This observation was seen for both genome-filled and empty capsids. Additionally, the percentage of empty particles in micrographs of capsids with or without integrin was similar. Taken together, these results implies that the integrin αvβ6 acts as an attachment receptor only and further receptors for entry and uncoating are required for destabilizing the capsid and RNA release. Such distinction between attachment and entry receptors has been reported for three other picornaviruses: CVB3, CVA21, and echovirus 1 (Shafren *et al.* 1997, Xing *et al.* 2004, Milstone *et al.* 2005). Such a multi-step process for RNA uncoating by a virus could be useful for escaping the humoral immune response because different receptors may recognize different regions on the capsid so that blocking of an epitope by an antibody may not abort infection. Additionally, such a multi-step process could also be important to ensure that the virus genome is delivered to the correct part of the cell for viral genome replication.

Does RNA encode clues for pathogenesis and tropism differences among viral strains?

For many viruses, such as the CVA7 strains in study I, different strains show difference in tropism and pathogenesis. CVA7 Parker and USSR strains presented with acute flaccid paralysis in human and were pathogenic in suckling mice whereas CVA7 275/58 caused aseptic meningitis in humans but was non-pathogenic in suckling mice (Habel and Loomis 1957, Grist 1962, Richter *et al.* 1971). We carried out nucleotide sequencing of the capsid protein coding regions of CAV7 USSR and 275/58 strains and compared them to the

CAV7 Parker. This showed that the 275/58 strain was more distant from the Parker strain with ~82% nucleotide sequence similarity and about 96% amino acid sequence similarity. The USSR strains was nearly identical to the Parker strain with about 99.5% nucleotide sequence similarity and about 99% amino acid sequence similarity even though the Parker strain originated in the USA whereas the USSR originated in the former Soviet Union. In fact, these sequence variations held true when the whole genome of Parker, USSR and 275/58 strains were sequenced recently showing Parker and USSR strains to be nearly identical whereas 82.6% nucleotide sequence variation and 96.2% amino acid variation was found between 275/58 and Parker strain (Ylä-Pelto *et al.* 2013).

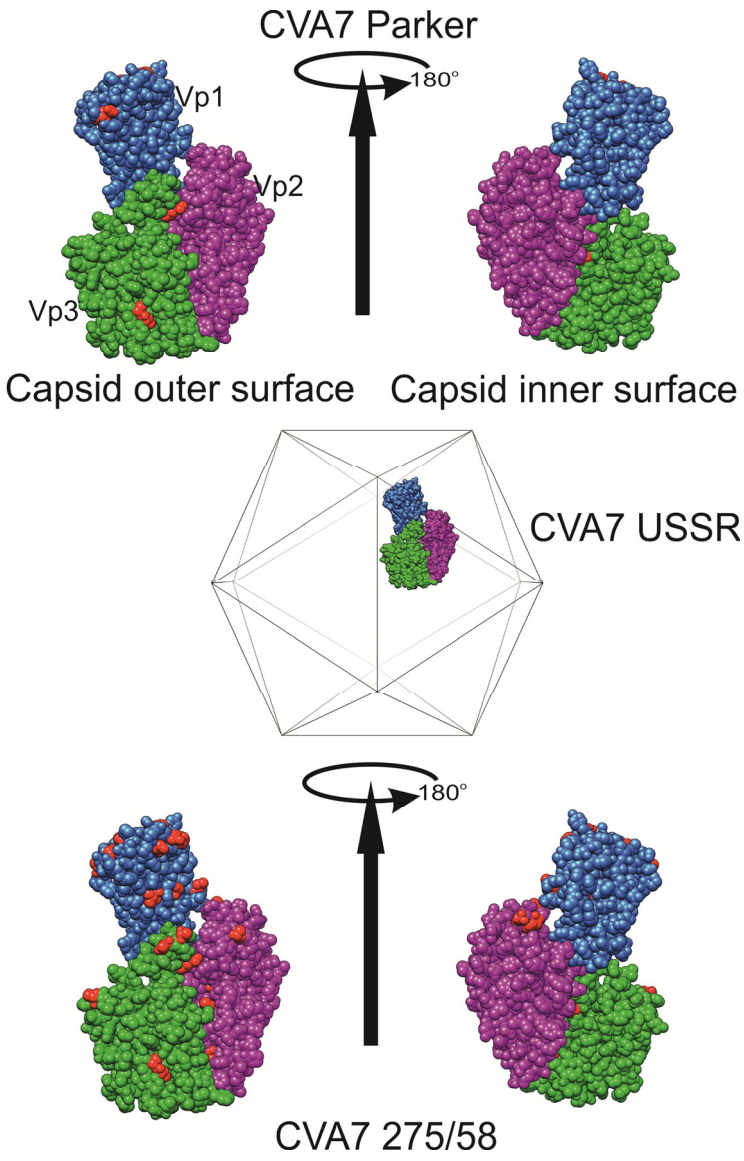

Figure 8. CVA7 capsid surface variations.

The CVA7 Parker and 275/58 strains amino acid sequences were aligned to CVA7 USSR strains. The variations in residues (red) were mapped on the pseudo-atomic CVA7 USSR capsid model.

Apparently, these amino acid variations in CVA7 strains were not found in linear regions but were distributed randomly throughout the sequence. Mapping the Parker and 275/58 strain variations on the capsid surface residues of CVA7 USSR pseudo-atomic models showed that variability on VP1's surface accounted for most of the difference between the strains (Figure 8). These capsid surface variations could be the cause of distinct infections by CVA7 strains and represent hyper-variable regions in the viral RNA genome. Such a difference in pathogenesis and tropism of CVA7 is reminiscent of what is seen in tissue tropism of coxsackievirus subgroup A and B where coxsackievirus subgroup A sites of infection were heart and skeletal muscles in mice whereas subgroup B had broader tissue tropism and were found in the central nervous system, pancreas, brown fat and liver of the mice (Hyypiä *et al.* 1993).

4.2. Viral RNA guided assembly

Does the picornavirus RNA genome have packaging signals (PSs) for capsid assembly? This is a long-standing question in the field. In order to investigate this issue, HPeV1 was utilized, as a previous 3-D reconstruction (EMDB: 1690) had shown strong ordered density not only for the capsid, but also for the RNA, especially where the two met on the inner surface of the capsid (Seitsonen *et al.* 2010). No empty capsids were enriched in any fractions from the cesium chloride gradient used for virus purification unlike other picornaviruses for e.g. study I and II of this thesis where the virus band on the gradient contained genome-filled as well as empty capsids. These observations indicate that there is a strong association between the HPeV1 capsid proteins and the viral RNA resulting in very efficient assembly and packaging. In order to understand this association and to identify PSs on viral RNA, the HPeV1

Harris strain capsids were heat-dissociated into pentamers which have been shown to be the building blocks of capsid assembly by *in vitro* assembly assays on bovine enterovirus (Li *et al.* 2012). These pentamers were panned on to an artificial random library of 40mer RNA aptamers using systematic evolution of ligands by exponential enrichment (SELEX) (Tuerk and Gold 1990), in an approach similar to one that had been used for STNV (Bunka *et al.* 2011). SELEX is a technique developed to enrich functional moieties (aptamers) from a vast variety of DNA or RNA libraries generated randomly with enough diversity that it actual contains at least one of the possible functional moieties that we are hunting for (Joyce 1989, Ellington and Szostak 1990, Tuerk and Gold 1990). The screening for aptamers against HPeV1 pentamers was done by alternating between positive selection with pentamers and negative selection with undisrupted capsids and naked streptavidin beads. The 13^{th} round aptamers were amplified by polymerase chain reaction and sequenced.

By aligning 423,932 unique sequences identified by next generation sequencing (NGS) to the HPeV1 Harris genome (Genbank ID: L02971) (Hyypiä *et al.* 1992) using an in-house alignment strategy, the five most frequently aligned aptamer sequences were identified. The alignment of the aptamers to the genome was assessed by a Bernoulli score which was generated by calculating the probability of having a number of mismatches between the aptamers and the genome over a length of 40 nucleotides. The alignment of an aptamer was considered significant when the Bernoulli score was 12 or more because a score of less than 12 could occur just by taking a random sequence of 40 nucleotides in length. This alignment of each aptamer sequence to any possible contiguous genomic fragment of 40 nucleotides in length in the Harris genome was done by sliding the aptamer sequence in 1 nucleotide increments

along the genome resulting in a series of comparison frames. Additionally, alignment of at least 12 nucleotides length of the 5' end of the aptamer sequence with the 3' end of the genomic sequence and vice-versa, were also considered so that information from the 5'- and 3'-ends was not missed, in case the genome present itself in a circular form to the pentamers. In particular, we started the alignment procedure by aligning the last nucleotide of the aptamer sequence with the first nucleotide at the 5' end of the genome. The aligned aptamer sequences and the corresponding HPeV1 Harris genome sequences were folded *in silico* to identify those containing potential stem-loops using the MFOLD program (Zuker 2003). The alignment showed nucleotides 1500-2250 (capsid protein VP1 coding region) and nucleotides 6000-6750 (RNA-dependent RNA-polymerase coding region) on the genome as the regions with the highest Bernoulli score of 17/18. However, the majority of the aptamers were found to align to the 3' UTR region but with a lower Bernoulli score.

In order to test whether the identified alignment hit regions were conserved across different strains of HPeV1; the 21 fully-sequenced strains of HPeV1 available in Genbank were aligned to each other. This alignment was done by initially dividing the genome sequences into 5' UTR, coding region and 3' UTR. The 5' UTR and 3' UTR nucleotide sequences and the translated coding region regions were aligned using Clustal-Omega (Sievers *et al.* 2011). The alignment of translated coding region was further improved by using PAL2NAL (Suyama *et al.* 2006) which does the nucleotide alignment using the amino acid alignment as the constraint. Finally, the alignment of 5' UTR, coding region and 3' UTR were assembled together to obtain the alignment of the full-length genomes. Comparison of these 21 aligned genome sequences to the alignment of aptamers to the Harris genome showed that the identified

alignment hit regions were relatively conserved compared to the rest of the genome. The genome regions with hits of the highest possible Bernoulli scores of 17 or 18 were folded into stem-loop structures by Mfold (Zuker 2003). Those folds which showed strongest similarity with the folds of the five most abundant aptamers returned by SELEX were chosen as the putative PSs. Nucleotide alignment of these PSs using ClustalW (Larkin *et al.* 2007) indicated a poly-uridine based common sequence motif.

A thermophoresis-based binding study on one of the putative PSs with isolated HPeV1 pentamers gave 12.5 nanomolar affinity. Hence this is preliminary evidence that there are selective, high affinity interactions between the HPeV1 genome and its capsid.

Looking at the geometry of these RNA-capsid interactions in the EM map, 5 PSs per pentamer and maximally 60 PSs for the whole capsid were expected. Our bioinformatics analysis identified 44 occurrences of the poly-uridine based PSs distributed throughout the genome. Comparatively, MS2 and GA bacteriophage (T=3) have multiple PSs distributed at 25 and 23 positions throughout the genome and the STNV (T=1) has 30 occurrence of the PSs motif in its genome (Dykeman *et al.* 2013). The expectation, given the identification of these PSs, is that the folding of the viral RNA is not a sequential process as with capsid assembly nucleating from one specific position on the genome, rather, RNA folding could be a 'collapse' where multiple specific PSs on the genome result in efficient co-assembly of pentamers and RNA into a 'virion' as has been seen for MS2 and STNV using smFSC (Borodavka *et al.* 2012, 2013, Stockley *et al.* 2013).

One may argue whether or not these PSs need to be specific to a virus type or can they be simple stem-loop structures. The comparison of MS2, GA

and STNV PSs showed that the stem-loop structural motif varies in both length and consensus sequence between the viruses. This variation indicates that viral RNAs have evolved to get specifically packaged into their specific capsids (Bunka *et al.* 2011, Dykeman *et al.* 2013). The assembly with non-specific PSs can still occur but will be far more inefficient (Borodavka *et al.* 2013).

In conclusion, the initial analysis of different HPeV strains indicates conservation of the PSs across different strains. This is not too surprising because these interactions are not under the same selection pressure from the host as the exposed regions of the capsid. There is a need to develop competitive assembly assays in order to test this hypothesis further. The results are encouraging as the basis for developing new antiviral drugs targeting virus assembly.

4.3. Improving model fitting in EM density maps

Study I on CVA7 utilized fitting of homology models derived from remote homologs into the EM density maps of genome-filled and empty capsids at sub-nanometer resolution of 6 and 8Å, respectively. The flexible fitting was performed by Flex-EM by running it in the simulated annealing molecular dynamics mode (Topf *et al.* 2008). The program treats secondary structure elements as rigid bodies and tries to fit them into the EM density maps. Some regions of the homology models were not fitted into the maps due to low confidence in homology modelling in those regions or ambiguous segmentation of the density maps especially at the subunit interfaces. For study II on CVA9, we fitted atomic models available from X-ray into the EM density maps of genome-filled and empty capsids around the resolution of 9Å using another flexible fitting program, iMODfit due to its higher computational speed

(Lopez-Blanco and Chacon 2013). It works by normal mode analysis where some dihedral angles are fixed and other are kept flexible.

Experience of working with two different flexible fitting programs led us to develop a generalized protocol for fitting homology models into EM density maps of icosahedral viruses and validating these fits (study III). The protocol begins with generation of homology models and their initial rigid fitting into the target EM density map followed by flexible fitting using Flex-EM and iMODfit programs. Regions of consensus and non-consensus fits between Flex-EM and iMODfit are identified by calculating Cα root mean square deviation (RMSD) between the fits from these two program and by segment cross correlation score (SCCC) estimation between the simulated map of the fit and its corresponding EM density map, followed by SCCC comparison for each segment between Flex-EM and iMODfit. The segment in SCCC can be a secondary structure element (SSE) like α-helices and β-sheets, or an individual protein of an assembly of proteins. Identified regions of non-consensus are further flexibly fitted using Flex-EM to improve the fit. Recently, such a protocol for identifying consensus and non-consensus region using multiple fitting programs has also been described elsewhere (Ahmed *et al.* 2012). Several important aspects related to fitting homology models into EM density maps are also highlighted in study III such as errors in homology modelling, segmentation difficulties, over-fitting, fitting one conformation of a model into the density map of a different conformation.

To explore the effect of the homology modelling errors that creep into the fitting, we made a homology model of actin using MODELLER (Sali and Blundell 1993) from actin-related protein 3 (Arp3) from an Arp2/3 complex (PDB: 1K8K, chain A) (Robinson *et al.* 2001) and fitted it into a 9Å resolution

EM density map derived from an actin atomic model (PDB: 2A40) (Chereau *et al.* 2005) using Flex-EM (Topf *et al.* 2008) and iMODfit (Lopez-Blanco and Chacon 2013). Comparing these fits against each other and against the crystal structure by Cα RMSD and SCCC showed regions for which the two flexible fitting programs did not have consensus fits. In addition, calculation of local residue error in the actin homology model using the QMEAN server (Benkert *et al.* 2009) identified six unreliable loop segments when a cut-off >3.5Å was used. The local residue error was calculated based on comparing the absolute quality of the query models to the high-resolution X-rays structures of similar size (Benkert *et al.* 2009). These loop segments were connected to the SSEs with low consensus fit between Flex-EM and iMODfit. Further refinement of the fit from iMODfit was done using Flex-EM by relaxing all the SSEs having lower SCCC values for iMODfit compared to Flex-EM. This refinement step using Flex-EM improved the fit only for helix 76-78 showing the errors of modelling could not be completely abolished during fitting.

Fitting models into macromolecular assemblies such as virus capsids comes with problems of fitting model of one conformation into a density map of another conformation, segmentation of individual capsid proteins and asymmetric units from the entire density map and issues of overfitting. To demonstrate these issues, we fitted a crystal structure of the EV71 genome filled capsid (PDB: 3VBF) (Wang *et al.* 2012) into an expanded procapsid EV71 EM density map (EMDB: 5557) (Cifuente *et al.* 2013) at 9Å resolution for which a corresponding crystal structure (PDB: 4GMP) was also available to serve as the target/reference model (Cifuente *et al.* 2013). The procapsid EM density map (EMDB: 5557) was segmented into an asymmetric unit by zoning 9Å around the EV71 crystal structure (PDB: 3VBU) asymmetric unit using the

Chimera 'zone' tool (Pettersen *et al.* 2004). The initial rigid fitting was done with the 'Fit in map' tool in Chimera followed by flexible fitting in Flex-EM and iMODfit. The SSEs Cα RMSD comparison between Flex-EM and iMODfit showed regions of consensus (<5Å difference in Cα RMSD) and non-consensus. These regions showed direct correlation with the regions in the target map (PDB: 4GMP) where Flex-EM and iMODfit consensus regions have lower Cα RMSD between the target model and fits from Flex-EM and iMODfit compared to the non-consensus regions. This was further validated by generating the whole virus capsid from the fits from Flex-EM and iMODfit where non-consensus regions (VP1 helices: 169-172; VP2 helices 126-128, 159-167) with >10Å difference in Cα RMSD between Flex-EM and iMODfit were found to be involved in clashes at the interfaces of the asymmetric unit with its neighbours. These regions at the interface of asymmetric unit represent the areas where the segmentation is difficult possibly because of intertwining of the proteins from adjacent asymmetric unit. The issue of overfitting was highlighted with the non-consensus fit for VP2 β-hairpin (strands: 83-87, 90-94) where the SCCC score was similar for both Flex-EM and iMODfit when compared with the target model but the Cα RMSD was significantly higher for iMODfit (11Å) in comparison to Flex-EM (4Å). The VP2 β-hairpin was possibly fitted incorrectly by iMODfit as this was a region with badly resolved neighbourhood densities. A hybrid final model was generated by refining those SSEs in Flex-EM which had lower SCCC values compared to the corresponding iMODfit SSEs.

After doing bench testing on actin and EV71, we performed flexible fitting on CVA7. The CVA7 homology models used in study I were generated from a series of 10 remote homologs where in the best cases, the sequence

identities were only 42% for VP1, 58% for VP2 and 52% for VP3. With the availability of crystal structures from a close homolog, EV71 (Wang *et al.* 2012) having sequence identity of 60% for VP1, 84% for VP2 and 76% for VP3 we were able to generate improved homology models by giving empty (PDB: 3VBO) and genome-filled EV71 crystal structures (PDB: 3VBF) as the templates in I-TASSER (Roy *et al.* 2010). On assessing these models by local residue error profile in the QMEAN server (Benkert *et al.* 2009), we found that the β-barrels and the C-termini of VP1, VP2 and VP3 had lower local residue error compared to the models used in study I. Although in the new models we removed the unreliable 1-73 N-terminus residues and 278-296 C-terminus residues from VP1 and 1-40 N-terminus residues from N-terminus of VP3, we still had 47 more residues in VP1 and 12 more in VP3 compared to the models in study I. The VP1, VP2 and VP3 were assembled into an asymmetric unit by superimposing them on the asymmetric units of EV71 (PDB: 3VBO used for empty capsid models superimposition; PDB: 3VBF used for genome-filled models superimposition) in order to minimize intra-subunit clashes and segmentation errors. This was followed by rigid fitting in the segmented densities of VP1, VP2 and VP3 from study I using the 'fit in map' tool in Chimera (Pettersen *et al.* 2004). The rigidly fitted asymmetric unit was then used to re-segment the CVA7 empty and genome-filled EM density maps by zoning with a radius of 0.9 nm around the asymmetric unit. This was followed by flexible fitting in the segmented maps using Flex-EM and iMODfit.

Fitting in CVA7 empty density map using Flex-EM and iMODfit gave similar fits for β-barrels of VP2 and VP3 based on SCCC values, however for VP1, Flex-EM was slightly better with a SCCC score of 0.62 than iMODfit with a SCCC value of 0.58. Furthermore, there were some helices and sheets in

VP1, VP2 and VP3 which were fitted poorly in Flex-EM compared to iMODfit and vice-versa based on SCCC values. Fitting results in the CVA7 genome-filled density map were comparable using both Flex-EM and iMODfit except for the VP2 β-hairpin as was seen in the EV71 fitting test case. This discrepancy between the two programs for the VP2 β-hairpin was identified from the Cα RMSD which was found to be relatively high at 4.9Å. Interestingly, the Cα RMSD of the VP2 β-hairpin between fits of empty and genome-filled CVA7 using Flex-EM were the same as the corresponding one for EV71 empty (PDB: 3VBO) and genome-filled (PDB: 3VBF) with a value of 4.4Å. This better fit of the VP2 β-hairpin with Flex-EM in case of CVA7 and EV71 fitting could be due to the two-stage refinement process used by it where initially the Flex-EM fitting is done for the models more conservatively by clustering together SSEs with closer contact into a single rigid body using the program RIBFIND (Pandurangan and Topf 2012). This is followed by relaxing all the SSEs as individual rigid bodies in second stage of refinement. This two-stage refinement has been shown to minimize over-fitting during flexible fitting (Pandurangan and Topf 2012). Finally, to arrive at the hybrid final model, all the SSEs which had poor SCCC values in Flex-EM compared to iMODfit were further refined in Flex-EM. The whole capsid was generated for empty and genome-filled capsid models by the 'oligomer generator' tool in VIPERdb (Carrillo-Tripp *et al.* 2009) and any inter subunit clashes were resolved using the Flex-EM conjugant gradient protocol (Topf *et al.* 2008). In terms of biology, the models of CVA7 from study I and III were still comparable, however, as the new models had fewer truncated residues there was less uncertainty for movement of subunits within densities, hence, the overall conformational changes observed between empty and genome-filled state were more moderate. Such a protocol is not only applicable for fitting

models into virus capsid map but can be extended to other types of density maps as we demonstrated in our actin test case. The protocol presented in this work is similar to the proposal given by Ahmed and Tama (Ahmed and Tama 2013) where they advocated for comparing fitting results from multiple fitting programs so that a consensus fit can be obtained, however, our protocol besides doing fitting from two different programs, also performs an important validation step of these fits based on local fits of models into the density maps.

5. CONCLUSIONS AND FUTURE STUDIES

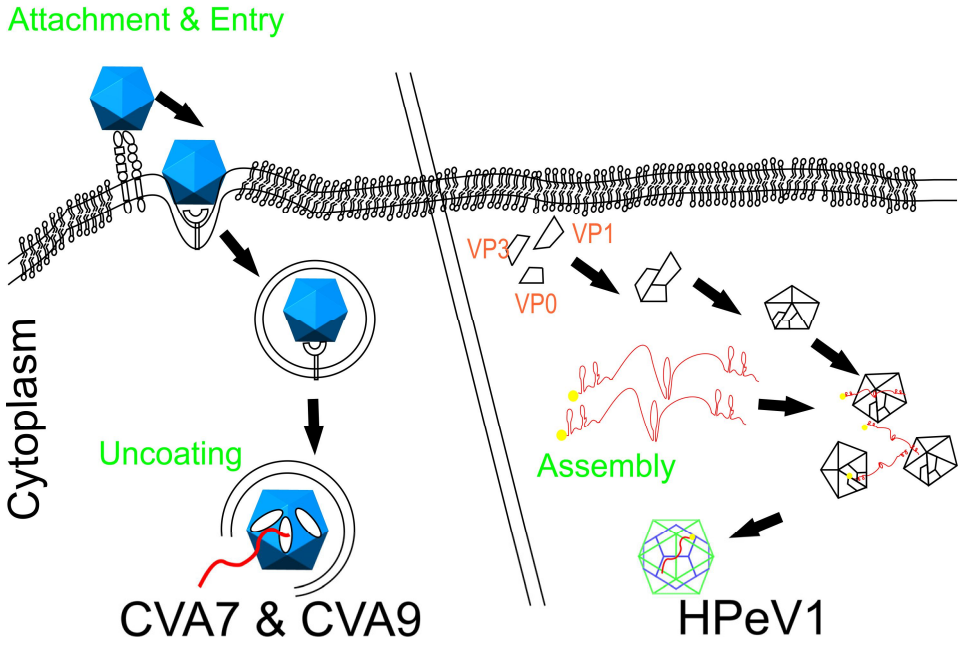

Figure 9. Schematic summary of thesis work.

A) CVA7 and CVA9 attachment, entry and uncoating. B) HPeV1 assembly.

The studies in this thesis along with recent work of others in the field have built a foundation for understanding the basic mechanisms of picornavirus entry and assembly (Figure 9). This thesis has elaborated the structural events associated with RNA egress by identification and quantification of concerted movements of capsid proteins between genome-filled and empty capsid state. These movements were mainly associated with translation of VP1 and rotation of VP2 and VP3 which resulted in opening of holes at the capsid with the largest ones at the two-fold symmetry axis which could be the sites for RNA release. Identification of these structural events were improved further by

designing of flexible fitting based protocol for fitting models derived from different complementary methods into the EM density maps. This work also elucidated the molecular mechanism of receptor-virus binding where structural evidence was provide for integrin αvβ6 functioning merely as an attachment receptor. Moreover, a functional role for RNA in assembly was also shown using HPeV1 as an example. Multiple PSs on RNA responsible for capsid assembly were identified using SELEX. These PSs had a poly-uridine based common motif.

But as is often the case in science, these findings gave rise to more questions than were originally answered. How does the virus choose just one exit point for the RNA out of 30 potential sites on the capsid and which is that site? How does a virus evolve to use cellular receptors as attachment or internalizing receptors? Apart from packaging signals on viral RNA, what other factors affect capsid assembly? In how many ways can viral co-assembly and packaging happen? Does the variation in surface capsid residues really cause the difference in pathogenesis and tropism *in vivo*? These are a few of the many questions on which we would like to work in the future.

Overall, this thesis provides several important targets such as the symmetry-related helices from two VP2 molecules in CVA7 and CVA9 or the RNA based PSs in HPeV1 which could be exploited for therapeutic potential.

6. ACKNOWLEDGEMENTS

This work was carried out between 2011 and 2013 at the Institute of Biotechnology and Department of Biosciences, University of Helsinki. This work was financed by Academy of Finland, Sigrid Juselius, Chancellor's travel grant and Helsinki Graduate Program in Biotechnology and Molecular Biology (GPBM) which is now merged into Integrated Life Science Doctoral Program (ILS).

I will begin the procession of 'thank you' with my supervisor Docent Sarah J. Butcher, Research Director of Structural Biology and Biophysics Programme at the Institute of Biotechnology. I am greatly indebted to her for providing me home away from home by accepting me in her lab as a Ph.D. student instead of technician position which I interviewed for. I wish to express my deepest gratitude to Sarah for being responsible for my holistic development as a scientist during my formative Ph.D. years. I thank her for her open door policy which I exploited quite a lot during my research by asking five minutes of her time which eventually ended in marathon sessions on scientific discussions. I thank her for hand-holding me during my transition period from being a molecular/cellular biologist into a structural virologist.

I would like to thank my co-supervisor Prof. Arto Urtti and thesis committee members, Prof. Adrian Goldman and Dr. Varpu Marjomäki for their critical comments during our meetings. I especially like to thank Adrian who is responsible for me ending up at Sarah's door step and for his constructive criticism during our group and thesis meetings.

I thank Petri Auvinen and José Castón for reviewing my thesis and for their critical comments. I thank David Stuart for finding time to be my opponent from his very busy schedule.

I like to thank all my co-authors and collaborators Jani Seitsonen, Petri Susi, Arun Pandurangan, Robert Sinkovits, Heini Hyvönen, Pasi Laurinmäki, Jani Ylä-Pelto, Maya Topf, Timo Hyypiä, Tommi Kajander, Eric Dykeman, Simon White, Ari Ora, Reidun Twarock and Peter Stockley without them this thesis would not have been possible. I especially like to thank Petri Susi for his helpful nature and providing me with any material whenever I asked him. I also like to thank our collaborators from London, Maya and Arun in whose lab I had a great time working on flexible fitting. I thoroughly enjoyed the company of Arun whenever we went to see Maya in Oxford. I extend my gratitude to Brenda and Katja for providing us with Human Parechovirus 1 and Susan Hafenstein for providing us with EV71 EM maps. I thank Giovanni Cardone for helpful suggestions about using AUTO3DEM and Jose R. Lopez-Blanco for assistance with iMODfit.

I would like to extend my deepest regards and thank you to all the 'Butcher arms' especially Ari, Lassi, Violeta, Veli-Pekka, Pasi, Lotta, Jani, Eevakaisa and Noha with whom I had maximum interaction and also Benita, Pezhman, Sergei and Riia.

Jani is thanked for building a great foundation for picornavirus work in our lab which had helped me immensely in carrying forward his work without any hiccups. I also thank him for all his help and guidance in image processing.

Ari Ora is thanked for being the second mentor to me after Sarah. He had been a great colleague, guide and especially a friend. He is a walking

encyclopedia of almost everything on earth and beyond. I had greatly enjoyed my long discussions with him on science, politics, economics, history, technology and life in general. He had given me tips and suggestions in almost all my experiments and I sincerely thank him for that. I thoroughly enjoyed doing experiments with him which always got extended to working really late in nights.

Lassi had been my office-mate and friend for the longest time. I am very thankful to him for maintaining the decorum and silence in our office which helped me in writing this thesis peacefully within the confines of our office. I really admire his great analytical thinking and problem solving skills in science and his wicked humor. For all the problems he has encountered during his Ph.D. he has always been able to come up with some smart solutions.

Violeta is one of the few friends I made in Finland and she is the first one with whom my social interaction started in Butcher lab. She is a great person to be around in the lab with never a dull moment. I admire her artistic and creative thinking and her helpful nature. She helped me to improve my listening skills and patience with her constant chattering.

Veli-Pekka had been a great colleague who had helped me with everything related to computers. Besides his programming skills, I greatly admire his legal counsel on every official matter.

I sincerely thank Pasi for introducing me to the work-horse of my research work, the Tecnai F20 electron microscope. Whatever little microscopy I have learned, I have learned it from him. I extend my gratitude to Eevakaisa as well for helping me with data collection and micrographs scanning.

My deepest regard and greatest gratitude goes to Arnab Kapat for recruiting me as a young research scientist in Reliance Life Science (RLS). I thank him for being my greatest inspiration to be a scientist. He is my mentor for life and he is solely responsible for me coming to foreign land to do my Ph.D. I also thank my immediate supervisor at RLS, Manoj Kumar and Venkata Ramana for introducing me to the field of therapeutic proteins, RNAi and viruses.

I would like to thank all my friends who have been great company to me throughout my life especially Imran, Muneer, Arif, Haja and Danish. I would also like to thank all the great friends I made at RLS, Bharat, Viddu, Shailendra, Murali, Sujoy, Bindu, Kriti and Shailaja. I also like to thank the Viikki cricket team for keeping me away from lab during beautiful Finnish summer evenings.

Most importantly I would like to thank my family for their unconditional love and support throughout my life. I would like to thank my late father, Dr. Shakeel and my mother, Seema for bringing me up in life with all the love and care a son can ask for. I warmly thank my elder brother, Zaki, for being more a father than a brother to me; I can never repay his love and support. I would like to extend my love to my younger siblings Saima, Kashish and Saani for all the fights and fun we had while growing up. I would also like to thank my sister-in-law, Nabeela and brother-in-law, Zafar for their support. My love to my nephew, Khalid and nieces, Minah and Simra.

I dedicate this thesis to Monica.

Helsinki, Finland March 2014

7. REFERENCES

Abed, Y. and Boivin, G. 2006. "Human parechovirus types 1, 2 and 3 infections in Canada." Emerg Infect Dis 12: 969-975.

Abrescia, N. G., Cockburn, J. J., Grimes, J. M., Sutton, G. C., Diprose, J. M., Butcher, S. J., Fuller, S. D., San Martin, C., Burnett, R. M., Stuart, D. I., Bamford, D. H. and Bamford, J. K. 2004. "Insights into assembly from structural analysis of bacteriophage PRD1." Nature 432: 68-74.

Acharya, R., Fry, E., Stuart, D., Fox, G., Rowlands, D. and Brown, F. 1989. "The three-dimensional structure of foot-and-mouth disease virus at 2.9 Å resolution." Nature 337: 709-716.

Adams, M. J., King, A. M. and Carstens, E. B. 2013. "Ratification vote on taxonomic proposals to the International Committee on Taxonomy of Viruses (2013)." Arch Virol 158: 2023-2030.

Ahmed, A. and Tama, F. 2013. "Consensus among multiple approaches as a reliability measure for flexible fitting into cryo-EM data." J Struct Biol 182: 67-77.

Ahmed, A., Whitford, P. C., Sanbonmatsu, K. Y. and Tama, F. 2012. "Consensus among flexible fitting approaches improves the interpretation of cryo-EM data." J Struct Biol 177: 561-570.

Alexander, H. E., Koch, G., Mountain, I. M. and Van Damme, O. 1958. "Infectivity of ribonucleic acid from poliovirus in human cell monolayers." J Exp Med 108: 493-506.

Ansardi, D. C., Porter, D. C. and Morrow, C. D. 1991. "Coinfection with recombinant vaccinia viruses expressing poliovirus P1 and P3 proteins results in polyprotein processing and formation of empty capsid structures." J Virol 65: 2088-2092.

Arnold, E. and Rossmann, M. G. 1990. "Analysis of the structure of a common cold virus, human rhinovirus 14, refined at a resolution of 3.0 Å." J Mol Biol 211: 763-801.

Atsumi, S., Matsumine, A., Toyoda, H., Niimi, R., Iino, T., Nakamura, T., Matsubara, T., Asanuma, K., Komada, Y., Uchida, A. and Sudo, A. 2012. "Oncolytic virotherapy for human bone and soft tissue sarcomas using live attenuated poliovirus." Int J Oncol 41: 893-902.

Baba, M. M., Oderinde, B. S., Patrick, P. Z. and Jarmai, M. M. 2012. "Sabin and wild polioviruses from apparently healthy primary school children in northeastern Nigeria." J Med Virol 84: 358-364.

Bai, X. C., Fernandez, I. S., McMullan, G. and Scheres, S. H. 2013. "Ribosome structures to near-atomic resolution from thirty thousand cryo-EM particles." Elife 2: e00461.

Baker, T. S. and Cheng, R. H. 1996. "A model-based approach for determining orientations of biological macromolecules imaged by cryoelectron microscopy." J Struct Biol 116: 120-130.

Baker, T. S., Olson, N. H. and Fuller, S. D. 1999. "Adding the third dimension to virus life cycles: three-dimensional reconstruction of icosahedral viruses from cryo-electron micrographs." Microbiol Mol Biol Rev 63: 862-922.

Barclay, W., Li, Q., Hutchinson, G., Moon, D., Richardson, A., Percy, N., Almond, J. W. and Evans, D. J. 1998. "Encapsidation studies of poliovirus subgenomic replicons." J Gen Virol 79 (Pt 7): 1725-1734.
Basavappa, R., Syed, R., Flore, O., Icenogle, J. P., Filman, D. J. and Hogle, J. M. 1994. "Role and mechanism of the maturation cleavage of VP0 in poliovirus assembly: structure of the empty capsid assembly intermediate at 2.9 Å resolution." Protein Sci 3: 1651-1669.
Basnak, G., Morton, V. L., Rolfsson, O., Stonehouse, N. J., Ashcroft, A. E. and Stockley, P. G. 2010. "Viral genomic single-stranded RNA directs the pathway toward a T=3 capsid." J Mol Biol 395: 924-936.
Beckett, D. and Uhlenbeck, O. C. 1988. "Ribonucleoprotein complexes of R17 coat protein and a translational operator analog." J Mol Biol 204: 927-938.
Beckett, D., Wu, H. N. and Uhlenbeck, O. C. 1988. "Roles of operator and non-operator RNA sequences in bacteriophage R17 capsid assembly." J Mol Biol 204: 939-947.
Bedard, K. M. and Semler, B. L. 2004. "Regulation of picornavirus gene expression." Microbes Infect 6: 702-713.
Bedke, N., Sammut, D., Green, B., Kehagia, V., Dennison, P., Jenkins, G., Tatler, A., Howarth, P. H., Holgate, S. T. and Davies, D. E. 2012. "Transforming growth factor-beta promotes rhinovirus replication in bronchial epithelial cells by suppressing the innate immune response." PLoS One 7: e44580.
Belnap, D. M., McDermott, B. M., Jr., Filman, D. J., Cheng, N., Trus, B. L., Zuccola, H. J., Racaniello, V. R., Hogle, J. M. and Steven, A. C. 2000a. "Three-dimensional structure of poliovirus receptor bound to poliovirus." Proc Natl Acad Sci U S A 97: 73-78.
Belnap, D. M., Filman, D. J., Trus, B. L., Cheng, N., Booy, F. P., Conway, J. F., Curry, S., Hiremath, C. N., Tsang, S. K., Steven, A. C. and Hogle, J. M. 2000b. "Molecular tectonic model of virus structural transitions: the putative cell entry states of poliovirus." J Virol 74: 1342-1354.
Benkert, P., Kunzli, M. and Schwede, T. 2009. "QMEAN server for protein model quality estimation." Nucleic Acids Res 37: W510-514.
Bergelson, J. M., Cunningham, J. A., Droguett, G., Kurt-Jones, E. A., Krithivas, A., Hong, J. S., Horwitz, M. S., Crowell, R. L. and Finberg, R. W. 1997. "Isolation of a common receptor for Coxsackie B viruses and adenoviruses 2 and 5." Science 275: 1320-1323.
Berinstein, A., Roivainen, M., Hovi, T., Mason, P. W. and Baxt, B. 1995. "Antibodies to the vitronectin receptor (integrin alpha V beta 3) inhibit binding and infection of foot-and-mouth disease virus to cultured cells." J Virol 69: 2664-2666.
Bjorndahl, T. C., Andrew, L. C., Semenchenko, V. and Wishart, D. S. 2007. "NMR solution structures of the apo and peptide-inhibited human rhinovirus 3C protease (Serotype 14): structural and dynamic comparison." Biochemistry 46: 12945-12958.
Boonyakiat, Y., Hughes, P. J., Ghazi, F. and Stanway, G. 2001. "Arginine-glycine-aspartic acid motif is critical for human parechovirus 1 entry." J Virol 75: 10000-10004.

Borodavka, A., Tuma, R. and Stockley, P. G. 2012. "Evidence that viral RNAs have evolved for efficient, two-stage packaging." Proc Natl Acad Sci U S A 109: 15769-15774.
Borodavka, A., Tuma, R. and Stockley, P. G. 2013. "A two-stage mechanism of viral RNA compaction revealed by single molecule fluorescence." RNA Biol 10: 481-489.
Bostina, M., Levy, H., Filman, D. J. and Hogle, J. M. 2011. "Poliovirus RNA is released from the capsid near a twofold symmetry axis." J Virol 85: 776-783.
Bozym, R. A., Patel, K., White, C., Cheung, K. H., Bergelson, J. M., Morosky, S. A. and Coyne, C. B. 2011. "Calcium signals and calpain-dependent necrosis are essential for release of coxsackievirus B from polarized intestinal epithelial cells." Mol Biol Cell 22: 3010-3021.
Briggs, J. A., Huiskonen, J. T., Fernando, K. V., Gilbert, R. J., Scotti, P., Butcher, S. J. and Fuller, S. D. 2005. "Classification and three-dimensional reconstruction of unevenly distributed or symmetry mismatched features of icosahedral particles." J Struct Biol 150: 332-339.
Brown, F., Sellers, R. F. and Stewart, D. L. 1958. "Infectivity of ribonucleic acid from mice and tissue culture infected with the virus of foot-and-mouth disease." Nature 182: 535-536.
Bubeck, D., Filman, D. J. and Hogle, J. M. 2005a. "Cryo-electron microscopy reconstruction of a poliovirus-receptor-membrane complex." Nat Struct Mol Biol 12: 615-618.
Bubeck, D., Filman, D. J., Cheng, N., Steven, A. C., Hogle, J. M. and Belnap, D. M. 2005b. "The structure of the poliovirus 135S cell entry intermediate at 10-Ångstrom resolution reveals the location of an externalized polypeptide that binds to membranes." J Virol 79: 7745-7755.
Bunka, D. H., Lane, S. W., Lane, C. L., Dykeman, E. C., Ford, R. J., Barker, A. M., Twarock, R., Phillips, S. E. and Stockley, P. G. 2011. "Degenerate RNA packaging signals in the genome of Satellite Tobacco Necrosis Virus: implications for the assembly of a T=1 capsid." J Mol Biol 413: 51-65.
Butler, P. J. and Klug, A. 1971. "Assembly of the particle of tobacco mosaic virus from RNA and disks of protein." Nat New Biol 229: 47-50.
Cabrerizo, M., Tarrago, D., Munoz-Almagro, C., Del Amo, E., Dominguez-Gil, M., Eiros, J. M., Lopez-Miragaya, I., Perez, C., Reina, J., Otero, A., Gonzalez, I., Echevarria, J. E. and Trallero, G. 2013. "Molecular epidemiology of enterovirus 71, coxsackievirus A16 and A6 associated with hand, foot and mouth disease in Spain." Clin Microbiol Infect.
Callahan, P. L., Mizutani, S. and Colonno, R. J. 1985. "Molecular cloning and complete sequence determination of RNA genome of human rhinovirus type 14." Proc Natl Acad Sci U S A 82: 732-736.
Campbell, M. G., Cheng, A., Brilot, A. F., Moeller, A., Lyumkis, D., Veesler, D., Pan, J., Harrison, S. C., Potter, C. S., Carragher, B. and Grigorieff, N. 2012. "Movies of ice-embedded particles enhance resolution in electron cryo-microscopy." Structure 20: 1823-1828.

Carrillo-Tripp, M., Shepherd, C. M., Borelli, I. A., Venkataraman, S., Lander, G., Natarajan, P., Johnson, J. E., Brooks, C. L., 3rd and Reddy, V. S. 2009. "VIPERdb2: an enhanced and web API enabled relational database for structural virology." Nucleic Acids Res 37: D436-442.
Carroll, A. R., Rowlands, D. J. and Clarke, B. E. 1984. "The complete nucleotide sequence of the RNA coding for the primary translation product of foot and mouth disease virus." Nucleic Acids Res 12: 2461-2472.
Caspar, D. L. and Klug, A. 1962. "Physical principles in the construction of regular viruses." Cold Spring Harb Symp Quant Biol 27: 1-24.
Chen, J. Z., Settembre, E. C., Aoki, S. T., Zhang, X., Bellamy, A. R., Dormitzer, P. R., Harrison, S. C. and Grigorieff, N. 2009. "Molecular interactions in rotavirus assembly and uncoating seen by high-resolution cryo-EM." Proc Natl Acad Sci U S A 106: 10644-10648.
Chereau, D., Kerff, F., Graceffa, P., Grabarek, Z., Langsetmo, K. and Dominguez, R. 2005. "Actin-bound structures of Wiskott-Aldrich syndrome protein (WASP)-homology domain 2 and the implications for filament assembly." Proc Natl Acad Sci U S A 102: 16644-16649.
Choi, Y. G. and Rao, A. L. 2003. "Packaging of brome mosaic virus RNA3 is mediated through a bipartite signal." J Virol 77: 9750-9757.
Chumakov, M., Voroshilova, M., Shindarov, L., Lavrova, I., Gracheva, L., Koroleva, G., Vasilenko, S., Brodvarova, I., Nikolova, M., Gyurova, S., Gacheva, M., Mitov, G., Ninov, N., Tsylka, E., Robinson, I., Frolova, M., Bashkirtsev, V., Martiyanova, L. and Rodin, V. 1979. "Enterovirus 71 isolated from cases of epidemic poliomyelitis-like disease in Bulgaria." Arch Virol 60: 329-340.
Chung, C. Y., Chen, C. Y., Lin, S. Y., Chung, Y. C., Chiu, H. Y., Chi, W. K., Lin, Y. L., Chiang, B. L., Chen, W. J. and Hu, Y. C. 2010. "Enterovirus 71 virus-like particle vaccine: improved production conditions for enhanced yield." Vaccine 28: 6951-6957.
Cifuente, J. O., Lee, H., Yoder, J. D., Shingler, K. L., Carnegie, M. S., Yoder, J. L., Ashley, R. E., Makhov, A. M., Conway, J. F. and Hafenstein, S. 2013. "Structures of the procapsid and mature virion of enterovirus 71 strain 1095." J Virol 87: 7637-7645.
Clements, G. B., Galbraith, D. N. and Taylor, K. W. 1995. "Coxsackie B virus infection and onset of childhood diabetes." Lancet 346: 221-223.
Cockburn, J. J., Abrescia, N. G., Grimes, J. M., Sutton, G. C., Diprose, J. M., Benevides, J. M., Thomas, G. J., Jr., Bamford, J. K., Bamford, D. H. and Stuart, D. I. 2004. "Membrane structure and interactions with protein and DNA in bacteriophage PRD1." Nature 432: 122-125.
Colter, J. S., Bird, H. H. and Brown, R. A. 1957. "Infectivity of ribonucleic acid from Ehrlich ascites tumour cells infected with Mengo encephalitis." Nature 179: 859-860.
Convery, M. A., Rowsell, S., Stonehouse, N. J., Ellington, A. D., Hirao, I., Murray, J. B., Peabody, D. S., Phillips, S. E. and Stockley, P. G. 1998. "Crystal structure of an RNA aptamer-protein complex at 2.8 Å resolution." Nat Struct Biol 5: 133-139.
Corrias, M. V., Flore, O., Broi, E., Marongiu, M. E., Pani, A., Torelli, S. and La Colla, P. 1987. "Characterization and role in morphogenesis of a new subviral particle (55S) isolated from poliovirus-infected cells." J Virol 61: 561-569.

Crick, F. H. and Watson, J. D. 1956. "Structure of small viruses." Nature 177: 473-475.
Crowther, R. A. 1971. "Procedures for three-dimensional reconstruction of spherical viruses by Fourier synthesis from electron micrographs." Philos Trans R Soc Lond B Biol Sci 261: 221-230.
Cui, A., Yu, D., Zhu, Z., Meng, L., Li, H., Liu, J., Liu, G., Mao, N. and Xu, W. 2010. "An outbreak of aseptic meningitis caused by coxsackievirus A9 in Gansu, the People's Republic of China." Virol J 7: 72.
Curry, S., Fry, E., Blakemore, W., Abu-Ghazaleh, R., Jackson, T., King, A., Lea, S., Newman, J. and Stuart, D. 1997. "Dissecting the roles of VP0 cleavage and RNA packaging in picornavirus capsid stabilization: the structure of empty capsids of foot-and-mouth disease virus." J Virol 71: 9743-9752.
Danthi, P., Tosteson, M., Li, Q. H. and Chow, M. 2003. "Genome delivery and ion channel properties are altered in VP4 mutants of poliovirus." J Virol 77: 5266-5274.
Davis, M. P., Bottley, G., Beales, L. P., Killington, R. A., Rowlands, D. J. and Tuthill, T. J. 2008. "Recombinant VP4 of human rhinovirus induces permeability in model membranes." J Virol 82: 4169-4174.
De Colibus, L., Wang, X., Spyrou, J. A., Kelly, J., Ren, J., Grimes, J., Puerstinger, G., Stonehouse, N., Walter, T. S., Hu, Z., Wang, J., Li, X., Peng, W., Rowlands, D. J., Fry, E. E., Rao, Z. and Stuart, D. I. 2014. "More-powerful virus inhibitors from structure-based analysis of HEV71 capsid-binding molecules." Nat Struct Mol Biol 21: 282-288.
De Rosier, D. J. and Klug, A. 1968. "Reconstruction of three dimensional structures from electron micrographs." Nature 217: 130-134.
Dent, K. C., Thompson, R., Barker, A. M., Hiscox, J. A., Barr, J. N., Stockley, P. G. and Ranson, N. A. 2013. "The asymmetric structure of an icosahedral virus bound to its receptor suggests a mechanism for genome release." Structure 21: 1225-1234.
Downing, K. H. 1995. "Progress in design and applications of CCD cameras for electron microscopy." Microscopy Today 95: 12.
Dubochet, J. M., A.W. 1981. "Vitrification of pure water for electron microscopy." J Microscopy 124: RP3-RP4.
Dykeman, E. C., Stockley, P. G. and Twarock, R. 2010. "Dynamic allostery controls coat protein conformer switching during MS2 phage assembly." J Mol Biol 395: 916-923.
Dykeman, E. C., Stockley, P. G. and Twarock, R. 2013. "Packaging signals in two single-stranded RNA viruses imply a conserved assembly mechanism and geometry of the packaged genome." J Mol Biol 425: 3235-3249.
Dykeman, E. C., Grayson, N. E., Toropova, K., Ranson, N. A., Stockley, P. G. and Twarock, R. 2011. "Simple rules for efficient assembly predict the layout of a packaged viral RNA." J Mol Biol 408: 399-407.
Ehrnst, A. and Eriksson, M. 1993. "Epidemiological features of type 22 echovirus infection." Scand J Infect Dis 25: 275-281.
Ellington, A. D. and Szostak, J. W. 1990. "In vitro selection of RNA molecules that bind specific ligands." Nature 346: 818-822.

Fabiola, F. and Chapman, M. S. 2005. "Fitting of high-resolution structures into electron microscopy reconstruction images." Structure 13: 389-400.
Faruqi, A. R. and Henderson, R. 2007. "Electronic detectors for electron microscopy." Curr Opin Struct Biol 17: 549-555.
Felli, I. C. and Pierattelli, R. 2012. "Recent progress in NMR spectroscopy: toward the study of intrinsically disordered proteins of increasing size and complexity." IUBMB Life 64: 473-481.
Filman, D. J., Syed, R., Chow, M., Macadam, A. J., Minor, P. D. and Hogle, J. M. 1989. "Structural factors that control conformational transitions and serotype specificity in type 3 poliovirus." EMBO J 8: 1567-1579.
Fischer, N., Konevega, A. L., Wintermeyer, W., Rodnina, M. V. and Stark, H. 2010. "Ribosome dynamics and tRNA movement by time-resolved electron cryomicroscopy." Nature 466: 329-333.
Fricks, C. E. and Hogle, J. M. 1990. "Cell-induced conformational change in poliovirus: externalization of the amino terminus of VP1 is responsible for liposome binding." J Virol 64: 1934-1945.
Fuller, S. D., Butcher, S. J., Cheng, R. H. and Baker, T. S. 1996. "Three-dimensional reconstruction of icosahedral particles--the uncommon line." J Struct Biol 116: 48-55.
Garriga, D., Pickl-Herk, A., Luque, D., Wruss, J., Caston, J. R., Blaas, D. and Verdaguer, N. 2012. "Insights into minor group rhinovirus uncoating: the X-ray structure of the HRV2 empty capsid." PLoS Pathog 8: e1002473.
Golmohammadi, R., Valegard, K., Fridborg, K. and Liljas, L. 1993. "The refined structure of bacteriophage MS2 at 2.8 Å resolution." J Mol Biol 234: 620-639.
Gottlieb, P., Strassman, J., Frucht, A., Qiao, X. Y. and Mindich, L. 1991. "In vitro packaging of the bacteriophage phi 6 ssRNA genomic precursors." Virology 181: 589-594.
Gottlieb, P., Strassman, J., Qiao, X., Frilander, M., Frucht, A. and Mindich, L. 1992. "In vitro packaging and replication of individual genomic segments of bacteriophage phi 6 RNA." J Virol 66: 2611-2616.
Greve, J. M., Davis, G., Meyer, A. M., Forte, C. P., Yost, S. C., Marlor, C. W., Kamarck, M. E. and McClelland, A. 1989. "The major human rhinovirus receptor is ICAM-1." Cell 56: 839-847.
Grigorieff, N. and Harrison, S. C. 2011. "Near-atomic resolution reconstructions of icosahedral viruses from electron cryo-microscopy." Curr Opin Struct Biol 21: 265-273.
Grimes, J. M., Jakana, J., Ghosh, M., Basak, A. K., Roy, P., Chiu, W., Stuart, D. I. and Prasad, B. V. 1997. "An atomic model of the outer layer of the bluetongue virus core derived from X-ray crystallography and electron cryomicroscopy." Structure 5: 885-893.
Grist, N. R. 1962. "Type A7 Coxsackie (type 4 poliomyelitis) virus infection in Scotland." J Hyg (Lond) 60: 323-332.
Grist, N. R., Bell, E. J. and Assaad, F. 1978. "Enteroviruses in human disease." Prog Med Virol 24: 114-157.

Gromeier, M., Alexander, L. and Wimmer, E. 1996. "Internal ribosomal entry site substitution eliminates neurovirulence in intergeneric poliovirus recombinants." Proc Natl Acad Sci U S A 93: 2370-2375.
Habel, K. and Loomis, L. N. 1957. "Coxsackie A7 virus and the Russian poliovirus Type 4." Proc Soc Exp Biol Med 95: 597-605.
Hadfield, A. T., Lee, W., Zhao, R., Oliveira, M. A., Minor, I., Rueckert, R. R. and Rossmann, M. G. 1997. "The refined structure of human rhinovirus 16 at 2.15 Å resolution: implications for the viral life cycle." Structure 5: 427-441.
Hafenstein, S., Palermo, L. M., Kostyuchenko, V. A., Xiao, C., Morais, M. C., Nelson, C. D., Bowman, V. D., Battisti, A. J., Chipman, P. R., Parrish, C. R. and Rossmann, M. G. 2007. "Asymmetric binding of transferrin receptor to parvovirus capsids." Proc Natl Acad Sci U S A 104: 6585-6589.
Hagiwara, A., Tagaya, I. and Yoneyama, T. 1978. "Epidemic of hand, foot and mouth disease associated with enterovirus 71 infection." Intervirology 9: 60-63.
He, Y., Bowman, V. D., Mueller, S., Bator, C. M., Bella, J., Peng, X., Baker, T. S., Wimmer, E., Kuhn, R. J. and Rossmann, M. G. 2000. "Interaction of the poliovirus receptor with poliovirus." Proc Natl Acad Sci U S A 97: 79-84.
He, Y., Chipman, P. R., Howitt, J., Bator, C. M., Whitt, M. A., Baker, T. S., Kuhn, R. J., Anderson, C. W., Freimuth, P. and Rossmann, M. G. 2001. "Interaction of coxsackievirus B3 with the full length coxsackievirus-adenovirus receptor." Nat Struct Biol 8: 874-878.
Heikkilä, O., Susi, P., Stanway, G. and Hyypiä, T. 2009. "Integrin alphaVbeta6 is a high-affinity receptor for coxsackievirus A9." J Gen Virol 90: 197-204.
Henderson, R. J. 1969. "The outbreak of foot-and-mouth disease in Worcestershire. An epidemiological study: with special reference to spread of the disease by wind-carriage of the virus." J Hyg (Lond) 67: 21-33.
Hendry, E., Hatanaka, H., Fry, E., Smyth, M., Tate, J., Stanway, G., Santti, J., Maaronen, M., Hyypiä, T. and Stuart, D. 1999. "The crystal structure of coxsackievirus A9: new insights into the uncoating mechanisms of enteroviruses." Structure 7: 1527-1538.
Hewat, E. A. and Blaas, D. 2004. "Cryoelectron microscopy analysis of the structural changes associated with human rhinovirus type 14 uncoating." J Virol 78: 2935-2942.
Hewat, E. A., Neumann, E. and Blaas, D. 2002. "The concerted conformational changes during human rhinovirus 2 uncoating." Mol Cell 10: 317-326.
Hewat, E. A., Neumann, E., Conway, J. F., Moser, R., Ronacher, B., Marlovits, T. C. and Blaas, D. 2000. "The cellular receptor to human rhinovirus 2 binds around the 5-fold axis and not in the canyon: a structural view." EMBO J 19: 6317-6325.
Hogle, J. M., Chow, M. and Filman, D. J. 1985. "Three-dimensional structure of poliovirus at 2.9 Å resolution." Science 229: 1358-1365.
Hohn, T. 1976. "Packaging of genomes in bacteriophages: a comparison of ssRNA bacteriophages and dsDNA bacteriophages." Philos Trans R Soc Lond B Biol Sci 276: 143-150.

Holland, J. J. and Kiehn, E. D. 1968. "Specific cleavage of viral proteins as steps in the synthesis and maturation of enteroviruses." Proc Natl Acad Sci U S A 60: 1015-1022.
Horn, W. T., Convery, M. A., Stonehouse, N. J., Adams, C. J., Liljas, L., Phillips, S. E. and Stockley, P. G. 2004. "The crystal structure of a high affinity RNA stem-loop complexed with the bacteriophage MS2 capsid: further challenges in the modeling of ligand-RNA interactions." RNA 10: 1776-1782.
Howe, C. L., Lafrance-Corey, R. G., Sundsbak, R. S. and Lafrance, S. J. 2012a. "Inflammatory monocytes damage the hippocampus during acute picornavirus infection of the brain." J Neuroinflammation 9: 50.
Howe, C. L., Lafrance-Corey, R. G., Sundsbak, R. S., Sauer, B. M., Lafrance, S. J., Buenz, E. J. and Schmalstieg, W. F. 2012b. "Hippocampal protection in mice with an attenuated inflammatory monocyte response to acute CNS picornavirus infection." Sci Rep 2: 545.
Hsieh, P. K., Chang, S. C., Huang, C. C., Lee, T. T., Hsiao, C. W., Kou, Y. H., Chen, I. Y., Chang, C. K., Huang, T. H. and Chang, M. F. 2005. "Assembly of severe acute respiratory syndrome coronavirus RNA packaging signal into virus-like particles is nucleocapsid dependent." J Virol 79: 13848-13855.
Hughes, P. J., Horsnell, C., Hyypiä, T. and Stanway, G. 1995. "The coxsackievirus A9 RGD motif is not essential for virus viability." J Virol 69: 8035-8040.
Huiskonen, J. T., Jäälinoja, H. T., Briggs, J. A., Fuller, S. D. and Butcher, S. J. 2007. "Structure of a hexameric RNA packaging motor in a viral polymerase complex." J Struct Biol 158: 156-164.
Huttenlocher, A. and Horwitz, A. R. 2011. "Integrins in cell migration." Cold Spring Harb Perspect Biol 3: a005074.
Hyypiä, T., Kallajoki, M., Maaronen, M., Stanway, G., Kandolf, R., Auvinen, P. and Kalimo, H. 1993. "Pathogenetic differences between coxsackie A and B virus infections in newborn mice." Virus Res 27: 71-78.
Hyypiä, T., Horsnell, C., Maaronen, M., Khan, M., Kalkkinen, N., Auvinen, P., Kinnunen, L. and Stanway, G. 1992. "A distinct picornavirus group identified by sequence analysis." Proc Natl Acad Sci U S A 89: 8847-8851.
Jackson, T., Sheppard, D., Denyer, M., Blakemore, W. and King, A. M. 2000. "The epithelial integrin alphavbeta6 is a receptor for foot-and-mouth disease virus." J Virol 74: 4949-4956.
Jackson, T., Ellard, F. M., Ghazaleh, R. A., Brookes, S. M., Blakemore, W. E., Corteyn, A. H., Stuart, D. I., Newman, J. W. and King, A. M. 1996. "Efficient infection of cells in culture by type O foot-and-mouth disease virus requires binding to cell surface heparan sulfate." J Virol 70: 5282-5287.
Jacobson, M. F. and Baltimore, D. 1968. "Polypeptide cleavages in the formation of poliovirus proteins." Proc Natl Acad Sci U S A 61: 77-84.
Jang, S. K., Krausslich, H. G., Nicklin, M. J., Duke, G. M., Palmenberg, A. C. and Wimmer, E. 1988. "A segment of the 5' nontranslated region of encephalomyocarditis virus RNA directs internal entry of ribosomes during in vitro translation." J Virol 62: 2636-2643.

Jia, Q., Liang, F., Ohka, S., Nomoto, A. and Hashikawa, T. 2002. "Expression of brain-derived neurotrophic factor in the central nervous system of mice using a poliovirus-based vector." J Neurovirol 8: 14-23.
Jia, X. Y., Van Eden, M., Busch, M. G., Ehrenfeld, E. and Summers, D. F. 1998. "Trans-encapsidation of a poliovirus replicon by different picornavirus capsid proteins." J Virol 72: 7972-7977.
Johansen, L. K. and Morrow, C. D. 2000a. "The RNA encompassing the internal ribosome entry site in the poliovirus 5' nontranslated region enhances the encapsidation of genomic RNA." Virology 273: 391-399.
Johansen, L. K. and Morrow, C. D. 2000b. "Inherent instability of poliovirus genomes containing two internal ribosome entry site (IRES) elements supports a role for the IRES in encapsidation." J Virol 74: 8335-8342.
Johnson, V. H. and Semler, B. L. 1988. "Defined recombinants of poliovirus and coxsackievirus: sequence-specific deletions and functional substitutions in the 5'-noncoding regions of viral RNAs." Virology 162: 47-57.
Joki-Korpela, P., Marjomäki, V., Krogerus, C., Heino, J. and Hyypiä, T. 2001. "Entry of human parechovirus 1." J Virol 75: 1958-1967.
Jokinen, J., White, D. J., Salmela, M., Huhtala, M., Kapyla, J., Sipila, K., Puranen, J. S., Nissinen, L., Kankaanpaa, P., Marjomäki, V., Hyypiä, T., Johnson, M. S. and Heino, J. 2010. "Molecular mechanism of alpha2beta1 integrin interaction with human echovirus 1." EMBO J 29: 196-208.
Jore, J. P., Veldhuisen, G., Pouwels, P. H., Boeye, A., Vrijsen, R. and Rombaut, B. 1991. "Formation of subviral particles by in vitro translation of subgenomic poliovirus RNAs." J Gen Virol 72 (Pt 11): 2721-2726.
Joyce, G. F. 1989. "Amplification, mutation and selection of catalytic RNA." Gene 82: 83-87.
Jäälinoja, H. T., Roine, E., Laurinmaki, P., Kivela, H. M., Bamford, D. H. and Butcher, S. J. 2008. "Structure and host-cell interaction of SH1, a membrane-containing, halophilic euryarchaeal virus." Proc Natl Acad Sci U S A 105: 8008-8013.
Karnauchow, T. M., Dawe, S., Lublin, D. M. and Dimock, K. 1998. "Short consensus repeat domain 1 of decay-accelerating factor is required for enterovirus 70 binding." J Virol 72: 9380-9383.
Katpally, U., Fu, T. M., Freed, D. C., Casimiro, D. R. and Smith, T. J. 2009. "Antibodies to the buried N terminus of rhinovirus VP4 exhibit cross-serotypic neutralization." J Virol 83: 7040-7048.
Kim, D. S., Kim, H., Shim, S. H., Kim, C., Song, M., Kim, Y. H., Jung, Y. W. and Nam, J. H. 2012. "Coxsackievirus B3 used as a gene therapy vector to express functional FGF2." Gene Ther 19: 1159-1165.
Kim, K. H., Willingmann, P., Gong, Z. X., Kremer, M. J., Chapman, M. S., Minor, I., Oliveira, M. A., Rossmann, M. G., Andries, K., Diana, G. D. and et al. 1993. "A comparison of the anti-rhinoviral drug binding pocket in HRV14 and HRV1A." J Mol Biol 230: 206-227.
Kitamura, N., Semler, B. L., Rothberg, P. G., Larsen, G. R., Adler, C. J., Dorner, A. J., Emini, E. A., Hanecak, R., Lee, J. J., van der Werf, S., Anderson, C. W. and Wimmer,

E. 1981. "Primary structure, gene organization and polypeptide expression of poliovirus RNA." Nature 291: 547-553.
Knight-Jones, T. J. and Rushton, J. 2013. "The economic impacts of foot and mouth disease - What are they, how big are they and where do they occur?" Prev Vet Med.
Kolatkar, P. R., Bella, J., Olson, N. H., Bator, C. M., Baker, T. S. and Rossmann, M. G. 1999. "Structural studies of two rhinovirus serotypes complexed with fragments of their cellular receptor." EMBO J 18: 6249-6259.
Koskiniemi, M., Paetau, R. and Linnavuori, K. 1989. "Severe encephalitis associated with disseminated echovirus 22 infection." Scand J Infect Dis 21: 463-466.
Krahn, P. M., O'Callaghan, R. J. and Paranchych, W. 1972. "Stages in phage R17 infection. VI. Injection of A protein and RNA into the host cell." Virology 47: 628-637.
Kumar, M. and Blaas, D. 2013. "Human rhinovirus subviral A particle binds to lipid membranes over a twofold axis of icosahedral symmetry." J Virol 87: 11309-11312.
Lander, G. C., Tang, L., Casjens, S. R., Gilcrease, E. B., Prevelige, P., Poliakov, A., Potter, C. S., Carragher, B. and Johnson, J. E. 2006. "The structure of an infectious P22 virion shows the signal for headful DNA packaging." Science 312: 1791-1795.
Larkin, M. A., Blackshields, G., Brown, N. P., Chenna, R., McGettigan, P. A., McWilliam, H., Valentin, F., Wallace, I. M., Wilm, A., Lopez, R., Thompson, J. D., Gibson, T. J. and Higgins, D. G. 2007. "Clustal W and Clustal X version 2.0." Bioinformatics 23: 2947-2948.
Legay, V., Chomel, J. J., Fernandez, E., Lina, B., Aymard, M. and Khalfan, S. 2002. "Encephalomyelitis due to human parechovirus type 1." J Clin Virol 25: 193-195.
Lever, A., Gottlinger, H., Haseltine, W. and Sodroski, J. 1989. "Identification of a sequence required for efficient packaging of human immunodeficiency virus type 1 RNA into virions." J Virol 63: 4085-4087.
Lewis, J. K., Bothner, B., Smith, T. J. and Siuzdak, G. 1998. "Antiviral agent blocks breathing of the common cold virus." Proc Natl Acad Sci U S A 95: 6774-6778.
Levy, H. C., Bostina, M., Filman, D. J. and Hogle, J. M. 2010. "Catching a virus in the act of RNA release: a novel poliovirus uncoating intermediate characterized by cryo-electron microscopy." J Virol 84: 4426-4441.
Li, C., Wang, J. C., Taylor, M. W. and Zlotnick, A. 2012. "In vitro assembly of an empty picornavirus capsid follows a dodecahedral path." J Virol 86: 13062-13069.
Li, Q., Yafal, A. G., Lee, Y. M., Hogle, J. and Chow, M. 1994. "Poliovirus neutralization by antibodies to internal epitopes of VP4 and VP1 results from reversible exposure of these sequences at physiological temperature." J Virol 68: 3965-3970.
Li, X., Mooney, P., Zheng, S., Booth, C. R., Braunfeld, M. B., Gubbens, S., Agard, D. A. and Cheng, Y. 2013. "Electron counting and beam-induced motion correction enable near-atomic-resolution single-particle cryo-EM." Nat Methods 10: 584-590.
Liao, M., Cao, E., Julius, D. and Cheng, Y. 2013. "Structure of the TRPV1 ion channel determined by electron cryo-microscopy." Nature 504: 107-112.

Lin, J., Lee, L. Y., Roivainen, M., Filman, D. J., Hogle, J. M. and Belnap, D. M. 2012. "Structure of the Fab-labeled "breathing" state of native poliovirus." J Virol 86: 5959-5962.
Lindert, S., Silvestry, M., Mullen, T. M., Nemerow, G. R. and Stewart, P. L. 2009. "Cryo-electron microscopy structure of an adenovirus-integrin complex indicates conformational changes in both penton base and integrin." J Virol 83: 11491-11501.
Liu, H., Jin, L., Koh, S. B., Atanasov, I., Schein, S., Wu, L. and Zhou, Z. H. 2010a. "Atomic structure of human adenovirus by cryo-EM reveals interactions among protein networks." Science 329: 1038-1043.
Liu, Y., Wang, C., Mueller, S., Paul, A. V., Wimmer, E. and Jiang, P. 2010b. "Direct interaction between two viral proteins, the nonstructural protein 2C and the capsid protein VP3, is required for enterovirus morphogenesis." PLoS Pathog 6: e1001066.
Liu, Z., Zhao, X., Mao, H., Baxter, P. A., Huang, Y., Yu, L., Wadhwa, L., Su, J. M., Adesina, A., Perlaky, L., Hurwitz, M., Idamakanti, N., Police, S. R., Hallenbeck, P. L., Hurwitz, R. L., Lau, C. C., Chintagumpala, M., Blaney, S. M. and Li, X. N. 2013. "Intravenous injection of oncolytic picornavirus SVV-001 prolongs animal survival in a panel of primary tumor-based orthotopic xenograft mouse models of pediatric glioma." Neuro Oncol 15: 1173-1185.
Lopez-Blanco, J. R. and Chacon, P. 2013. "iMODFIT: efficient and robust flexible fitting based on vibrational analysis in internal coordinates." J Struct Biol 184: 261-270.
Lu, H. H. and Wimmer, E. 1996. "Poliovirus chimeras replicating under the translational control of genetic elements of hepatitis C virus reveal unusual properties of the internal ribosomal entry site of hepatitis C virus." Proc Natl Acad Sci U S A 93: 1412-1417.
Maller, H. M., Powars, D. F., Horowitz, R. E. and Portnoy, B. 1967. "Fatal myocarditis associated with ECHO virus, type 22, infection in a child with apparent immunological deficiency." J Pediatr 71: 204-210.
Marongiu, M. E., Pani, A., Corrias, M. V., Sau, M. and La Colla, P. 1981. "Poliovirus morphogenesis. I. Identification of 80S dissociable particles and evidence for the artifactual production of procapsids." J Virol 39: 341-347.
McMullan, G., Chen, S., Henderson, R. and Faruqi, A. R. 2009. "Detective quantum efficiency of electron area detectors in electron microscopy." Ultramicroscopy 109: 1126-1143.
Mendelsohn, C. L., Wimmer, E. and Racaniello, V. R. 1989. "Cellular receptor for poliovirus: molecular cloning, nucleotide sequence, and expression of a new member of the immunoglobulin superfamily." Cell 56: 855-865.
Michos, A. G., Syriopoulou, V. P., Hadjichristodoulou, C., Daikos, G. L., Lagona, E., Douridas, P., Mostrou, G. and Theodoridou, M. 2007. "Aseptic meningitis in children: analysis of 506 cases." PLoS One 2: e674.
Milstone, A. M., Petrella, J., Sanchez, M. D., Mahmud, M., Whitbeck, J. C. and Bergelson, J. M. 2005. "Interaction with coxsackievirus and adenovirus receptor, but not with decay-accelerating factor (DAF), induces A-particle formation in a DAF-binding coxsackievirus B3 isolate." J Virol 79: 655-660.

Mindell, J. A. and Grigorieff, N. 2003. "Accurate determination of local defocus and specimen tilt in electron microscopy." J Struct Biol 142: 334-347.
Mindich, L. 2004. "Packaging, replication and recombination of the segmented genome of bacteriophage Phi6 and its relatives." Virus Res 101: 83-92.
Miyamoto, S., Inoue, H., Nakamura, T., Yamada, M., Sakamoto, C., Urata, Y., Okazaki, T., Marumoto, T., Takahashi, A., Takayama, K., Nakanishi, Y., Shimizu, H. and Tani, K. 2012. "Coxsackievirus B3 is an oncolytic virus with immunostimulatory properties that is active against lung adenocarcinoma." Cancer Res 72: 2609-2621.
Morais, M. C., Tao, Y., Olson, N. H., Grimes, S., Jardine, P. J., Anderson, D. L., Baker, T. S. and Rossmann, M. G. 2001. "Cryoelectron-microscopy image reconstruction of symmetry mismatches in bacteriophage phi29." J Struct Biol 135: 38-46.
Morales, L., Mateos-Gomez, P. A., Capiscol, C., del Palacio, L., Enjuanes, L. and Sola, I. 2013. "Transmissible gastroenteritis coronavirus genome packaging signal is located at the 5' end of the genome and promotes viral RNA incorporation into virions in a replication-independent process." J Virol 87: 11579-11590.
Morton, V. L., Dykeman, E. C., Stonehouse, N. J., Ashcroft, A. E., Twarock, R. and Stockley, P. G. 2010. "The impact of viral RNA on assembly pathway selection." J Mol Biol 401: 298-308.
Moschovi, M. A., Katsibardi, K., Theodoridou, M., Michos, A. G., Tsakris, A., Spanakis, N. and Tzortzatou-Stathopoulou, F. 2007. "Enteroviral infections in children with malignant disease: a 5-year study in a single institution." J Infect 54: 387-392.
Mu, Z., Wang, B., Zhang, X., Gao, X., Qin, B., Zhao, Z. and Cui, S. 2013. "Crystal structure of 2A proteinase from hand, foot and mouth disease virus." J Mol Biol 425: 4530-4543.
Muckelbauer, J. K., Kremer, M., Minor, I., Diana, G., Dutko, F. J., Groarke, J., Pevear, D. C. and Rossmann, M. G. 1995. "The structure of coxsackievirus B3 at 3.5 A resolution." Structure 3: 653-667.
Nathans, D., Oeschger, M. P., Eggen, K. and Shimura, Y. 1966. "Bacteriophage-specific proteins in e. Coli infected with an RNA bacteriophage." Proc Natl Acad Sci U S A 56: 1844-1851.
Nomoto, A., Detjen, B., Pozzatti, R. and Wimmer, E. 1977. "The location of the polio genome protein in viral RNAs and its implication for RNA synthesis." Nature 268: 208-213.
Nugent, C. I. and Kirkegaard, K. 1995. "RNA binding properties of poliovirus subviral particles." J Virol 69: 13-22.
Nugent, C. I., Johnson, K. L., Sarnow, P. and Kirkegaard, K. 1999. "Functional coupling between replication and packaging of poliovirus replicon RNA." J Virol 73: 427-435.
Ohka, S., Matsuda, N., Tohyama, K., Oda, T., Morikawa, M., Kuge, S. and Nomoto, A. 2004. "Receptor (CD155)-dependent endocytosis of poliovirus and retrograde axonal transport of the endosome." J Virol 78: 7186-7198.

Oliveira, M. A., Zhao, R., Lee, W. M., Kremer, M. J., Minor, I., Rueckert, R. R., Diana, G. D., Pevear, D. C., Dutko, F. J., McKinlay, M. A. and et al. 1993. "The structure of human rhinovirus 16." Structure 1: 51-68.
Olson, N. H., Kolatkar, P. R., Oliveira, M. A., Cheng, R. H., Greve, J. M., McClelland, A., Baker, T. S. and Rossmann, M. G. 1993. "Structure of a human rhinovirus complexed with its receptor molecule." Proc Natl Acad Sci U S A 90: 507-511.
Orlova, E. V. and Saibil, H. R. 2011. "Structural analysis of macromolecular assemblies by electron microscopy." Chem Rev 111: 7710-7748.
Paatero, A. O., Mindich, L. and Bamford, D. H. 1998. "Mutational analysis of the role of nucleoside triphosphatase P4 in the assembly of the RNA polymerase complex of bacteriophage phi6." J Virol 72: 10058-10065.
Pandurangan, A. P. and Topf, M. 2012. "RIBFIND: a web server for identifying rigid bodies in protein structures and to aid flexible fitting into cryo EM maps." Bioinformatics 28: 2391-2393.
Parent, K. N., Gilcrease, E. B., Casjens, S. R. and Baker, T. S. 2012. "Structural evolution of the P22-like phages: comparison of Sf6 and P22 procapsid and virion architectures." Virology 427: 177-188.
Paul, A. V., van Boom, J. H., Filippov, D. and Wimmer, E. 1998. "Protein-primed RNA synthesis by purified poliovirus RNA polymerase." Nature 393: 280-284.
Pelletier, J., Kaplan, G., Racaniello, V. R. and Sonenberg, N. 1988. "Cap-independent translation of poliovirus mRNA is conferred by sequence elements within the 5' noncoding region." Mol Cell Biol 8: 1103-1112.
Pettersen, E. F., Goddard, T. D., Huang, C. C., Couch, G. S., Greenblatt, D. M., Meng, E. C. and Ferrin, T. E. 2004. "UCSF Chimera--a visualization system for exploratory research and analysis." J Comput Chem 25: 1605-1612.
Pettersson, R. F., Ambros, V. and Baltimore, D. 1978. "Identification of a protein linked to nascent poliovirus RNA and to the polyuridylic acid of negative-strand RNA." J Virol 27: 357-365.
Pickl-Herk, A., Luque, D., Vives-Adrian, L., Querol-Audi, J., Garriga, D., Trus, B. L., Verdaguer, N., Blaas, D. and Caston, J. R. 2013. "Uncoating of common cold virus is preceded by RNA switching as determined by X-ray and cryo-EM analyses of the subviral A-particle." Proc Natl Acad Sci U S A 110: 20063-20068.
Pilipenko, E. V., Poperechny, K. V., Maslova, S. V., Melchers, W. J., Slot, H. J. and Agol, V. I. 1996. "Cis-element, oriR, involved in the initiation of (-) strand poliovirus RNA: a quasi-globular multi-domain RNA structure maintained by tertiary ('kissing') interactions." EMBO J 15: 5428-5436.
Pirttimaa, M. J. and Bamford, D. H. 2000. "RNA secondary structures of the bacteriophage phi6 packaging regions." RNA 6: 880-889.
Plevka, P., Perera, R., Cardosa, J., Kuhn, R. J. and Rossmann, M. G. 2012. "Crystal structure of human enterovirus 71." Science 336: 1274.
Plevka, P., Perera, R., Yap, M. L., Cardosa, J., Kuhn, R. J. and Rossmann, M. G. 2013. "Structure of human enterovirus 71 in complex with a capsid-binding inhibitor." Proc Natl Acad Sci U S A 110: 5463-5467.

Porta, C., Kotecha, A., Burman, A., Jackson, T., Ren, J., Loureiro, S., Jones, I. M., Fry, E. E., Stuart, D. I. and Charleston, B. 2013. "Rational engineering of recombinant picornavirus capsids to produce safe, protective vaccine antigen." PLoS Pathog 9: e1003255.
Porter, D. C., Ansardi, D. C. and Morrow, C. D. 1995. "Encapsidation of poliovirus replicons encoding the complete human immunodeficiency virus type 1 gag gene by using a complementation system which provides the P1 capsid protein in trans." J Virol 69: 1548-1555.
Porter, D. C., Ansardi, D. C., Wang, J., McPherson, S., Moldoveanu, Z. and Morrow, C. D. 1998. "Demonstration of the specificity of poliovirus encapsidation using a novel replicon which encodes enzymatically active firefly luciferase." Virology 243: 1-11.
Putnak, J. R. and Phillips, B. A. 1981. "Differences between poliovirus empty capsids formed in vivo and those formed in vitro: a role for the morphopoietic factor." J Virol 40: 173-183.
Qiao, X., Qiao, J. and Mindich, L. 2003. "Analysis of specific binding involved in genomic packaging of the double-stranded-RNA bacteriophage phi6." J Bacteriol 185: 6409-6414.
Qiao, X., Casini, G., Qiao, J. and Mindich, L. 1995. "In vitro packaging of individual genomic segments of bacteriophage phi 6 RNA: serial dependence relationships." J Virol 69: 2926-2931.
Qu, F. and Morris, T. J. 1997. "Encapsidation of turnip crinkle virus is defined by a specific packaging signal and RNA size." J Virol 71: 1428-1435.
Racaniello, V. R. and Baltimore, D. 1981. "Cloned poliovirus complementary DNA is infectious in mammalian cells." Science 214: 916-919.
Ramrath, D. J., Yamamoto, H., Rother, K., Wittek, D., Pech, M., Mielke, T., Loerke, J., Scheerer, P., Ivanov, P., Teraoka, Y., Shpanchenko, O., Nierhaus, K. H. and Spahn, C. M. 2012. "The complex of tmRNA-SmpB and EF-G on translocating ribosomes." Nature 485: 526-529.
Ranzenhofer, E. R., Dizon, F. C., Lipton, M. M. and Steigman, A. J. 1958. "Clinical paralytic poliomyelitis due to Coxsackie virus group A, type 7." N Engl J Med 259: 182.
Rastogi, S., Agarwal, A. K., Sipani, A. K., Varma, S. and Goel, M. K. 1983. "A clinical study of post polio infantile paralysis." Prosthet Orthot Int 7: 29-32.
Ren, J., Wang, X., Hu, Z., Gao, Q., Sun, Y., Li, X., Porta, C., Walter, T. S., Gilbert, R. J., Zhao, Y., Axford, D., Williams, M., McAuley, K., Rowlands, D. J., Yin, W., Wang, J., Stuart, D. I., Rao, Z. and Fry, E. E. 2013. "Picornavirus uncoating intermediate captured in atomic detail." Nat Commun 4: 1929.
Reuer, Q., Kuhn, R. J. and Wimmer, E. 1990. "Characterization of poliovirus clones containing lethal and nonlethal mutations in the genome-linked protein VPg." J Virol 64: 2967-2975.
Richter, F. A., Rhodes, A. J., Macpherson, L. W. and Labzoffsky, N. A. 1971. "A possible new enterovirus serotype isolated in Ontario." Arch Gesamte Virusforsch 35: 218-222.

Roberts, J. W. and Steitz, J. E. 1967. "The reconstitution of infective bacteriophage R17." Proc Natl Acad Sci U S A 58: 1416-1421.
Robinson, R. C., Turbedsky, K., Kaiser, D. A., Marchand, J. B., Higgs, H. N., Choe, S. and Pollard, T. D. 2001. "Crystal structure of Arp2/3 complex." Science 294: 1679-1684.
Roivainen, M., Piirainen, L. and Hovi, T. 1996. "Efficient RGD-independent entry process of coxsackievirus A9." Arch Virol 141: 1909-1919.
Roivainen, M., Hyypiä, T., Piirainen, L., Kalkkinen, N., Stanway, G. and Hovi, T. 1991. "RGD-dependent entry of coxsackievirus A9 into host cells and its bypass after cleavage of VP1 protein by intestinal proteases." J Virol 65: 4735-4740.
Roivainen, M., Piirainen, L., Hovi, T., Virtanen, I., Riikonen, T., Heino, J. and Hyypiä, T. 1994. "Entry of coxsackievirus A9 into host cells: specific interactions with alpha v beta 3 integrin, the vitronectin receptor." Virology 203: 357-365.
Roivainen, M., Knip, M., Hyoty, H., Kulmala, P., Hiltunen, M., Vahasalo, P., Hovi, T. and Akerblom, H. K. 1998. "Several different enterovirus serotypes can be associated with prediabetic autoimmune episodes and onset of overt IDDM. Childhood Diabetes in Finland (DiMe) Study Group." J Med Virol 56: 74-78.
Ross, T. D., Coon, B. G., Yun, S., Baeyens, N., Tanaka, K., Ouyang, M. and Schwartz, M. A. 2013. "Integrins in mechanotransduction." Curr Opin Cell Biol 25: 613-618.
Rossmann, M. G., He, Y. and Kuhn, R. J. 2002. "Picornavirus-receptor interactions." Trends Microbiol 10: 324-331.
Rossmann, M. G., Morais, M. C., Leiman, P. G. and Zhang, W. 2005. "Combining X-ray crystallography and electron microscopy." Structure 13: 355-362.
Rossmann, M. G., Arnold, E., Erickson, J. W., Frankenberger, E. A., Griffith, J. P., Hecht, H. J., Johnson, J. E., Kamer, G., Luo, M., Mosser, A. G. and et al. 1985. "Structure of a human common cold virus and functional relationship to other picornaviruses." Nature 317: 145-153.
Rowsell, S., Stonehouse, N. J., Convery, M. A., Adams, C. J., Ellington, A. D., Hirao, I., Peabody, D. S., Stockley, P. G. and Phillips, S. E. 1998. "Crystal structures of a series of RNA aptamers complexed to the same protein target." Nat Struct Biol 5: 970-975.
Roy, A., Kucukural, A. and Zhang, Y. 2010. "I-TASSER: a unified platform for automated protein structure and function prediction." Nat Protoc 5: 725-738.
Rueckert, R. R. and Wimmer, E. 1984. "Systematic nomenclature of picornavirus proteins." J Virol 50: 957-959.
Russell, S. J. and Bell, E. J. 1970. "Echoviruses and carditis." Lancet 1: 784-785.
Sali, A. and Blundell, T. L. 1993. "Comparative protein modelling by satisfaction of spatial restraints." J Mol Biol 234: 779-815.
Salmon, D. E. 1903. "The Present Outbreak of Foot-and-Mouth Disease in the New England States." J Mass Assoc Boards Health 13: 4-14.
San Martin, C., Burnett, R. M., de Haas, F., Heinkel, R., Rutten, T., Fuller, S. D., Butcher, S. J. and Bamford, D. H. 2001. "Combined EM/X-ray imaging yields a quasi-

atomic model of the adenovirus-related bacteriophage PRD1 and shows key capsid and membrane interactions." Structure 9: 917-930.
Sasaki, J. and Taniguchi, K. 2003. "The 5'-end sequence of the genome of Aichi virus, a picornavirus, contains an element critical for viral RNA encapsidation." J Virol 77: 3542-3548.
Schwarz, E. M., Badorff, C., Hiura, T. S., Wessely, R., Badorff, A., Verma, I. M. and Knowlton, K. U. 1998. "NF-kappaB-mediated inhibition of apoptosis is required for encephalomyocarditis virus virulence: a mechanism of resistance in p50 knockout mice." J Virol 72: 5654-5660.
Seitsonen, J., Susi, P., Heikkilä, O., Sinkovits, R. S., Laurinmäki, P., Hyypiä, T. and Butcher, S. J. 2010. "Interaction of alphaVbeta3 and alphaVbeta6 integrins with human parechovirus 1." J Virol 84: 8509-8519.
Semler, B. L. a. W., E., Ed. (2002). Molecular biology of picornaviruses, ASM Press, Washington DC.
Settembre, E. C., Chen, J. Z., Dormitzer, P. R., Grigorieff, N. and Harrison, S. C. 2011. "Atomic model of an infectious rotavirus particle." EMBO J 30: 408-416.
Shafren, D. R., Dorahy, D. J., Ingham, R. A., Burns, G. F. and Barry, R. D. 1997. "Coxsackievirus A21 binds to decay-accelerating factor but requires intercellular adhesion molecule 1 for cell entry." J Virol 71: 4736-4743.
Shafren, D. R., Bates, R. C., Agrez, M. V., Herd, R. L., Burns, G. F. and Barry, R. D. 1995. "Coxsackieviruses B1, B3, and B5 use decay accelerating factor as a receptor for cell attachment." J Virol 69: 3873-3877.
Shiba, T. and Suzuki, Y. 1981. "Localization of A protein in the RNA-A protein complex of RNA phage MS2." Biochim Biophys Acta 654: 249-255.
Shingler, K. L., Yoder, J. L., Carnegie, M. S., Ashley, R. E., Makhov, A. M., Conway, J. F. and Hafenstein, S. 2013. "The enterovirus 71 A-particle forms a gateway to allow genome release: a cryoEM study of picornavirus uncoating." PLoS Pathog 9: e1003240.
Sievers, F., Wilm, A., Dineen, D., Gibson, T. J., Karplus, K., Li, W., Lopez, R., McWilliam, H., Remmert, M., Söding, J., Thompson, J. D. and Higgins, D. G. 2011. "Fast, scalable generation of high-quality protein multiple sequence alignments using Clustal Omega." Mol Syst Biol 7: 539.
Smith, D. E., Tans, S. J., Smith, S. B., Grimes, S., Anderson, D. L. and Bustamante, C. 2001. "The bacteriophage straight phi29 portal motor can package DNA against a large internal force." Nature 413: 748-752.
Smyth, M., Tate, J., Hoey, E., Lyons, C., Martin, S. and Stuart, D. 1995. "Implications for viral uncoating from the structure of bovine enterovirus." Nat Struct Biol 2: 224-231.
Sperling, R., Koster, A. J., Melamed-Bessudo, C., Rubinstein, A., Angenitzki, M., Berkovitch-Yellin, Z. and Sperling, J. 1997. "Three-dimensional image reconstruction of large nuclear RNP (lnRNP) particles by automated electron tomography." J Mol Biol 267: 570-583.
Stanway, G. and Hyypiä, T. 1999. "Parechoviruses." J Virol 73: 5249-5254.

Stewart, P. L. and Nemerow, G. R. 2007. "Cell integrins: commonly used receptors for diverse viral pathogens." Trends Microbiol 15: 500-507.
Stewart, P. L., Burnett, R. M., Cyrklaff, M. and Fuller, S. D. 1991. "Image reconstruction reveals the complex molecular organization of adenovirus." Cell 67: 145-154.
Stockley, P. G., Rolfsson, O., Thompson, G. S., Basnak, G., Francese, S., Stonehouse, N. J., Homans, S. W. and Ashcroft, A. E. 2007. "A simple, RNA-mediated allosteric switch controls the pathway to formation of a T=3 viral capsid." J Mol Biol 369: 541-552.
Stockley, P. G., Twarock, R., Bakker, S. E., Barker, A. M., Borodavka, A., Dykeman, E., Ford, R. J., Pearson, A. R., Phillips, S. E., Ranson, N. A. and Tuma, R. 2013. "Packaging signals in single-stranded RNA viruses: nature's alternative to a purely electrostatic assembly mechanism." J Biol Phys 39: 277-287.
Streuli, C. H. 2009. "Integrins and cell-fate determination." J Cell Sci 122: 171-177.
Summers, D. F. and Maizel, J. V. 1968. "Evidence for Large Precursor Proteins in Poliovirus Synthesis." Proc Natl Acad Sci U S A 59: 966-&.
Suyama, M., Torrents, D. and Bork, P. 2006. "PAL2NAL: robust conversion of protein sequence alignments into the corresponding codon alignments." Nucleic Acids Res 34: W609-612.
Tao, Y., Olson, N. H., Xu, W., Anderson, D. L., Rossmann, M. G. and Baker, T. S. 1998. "Assembly of a tailed bacterial virus and its genome release studied in three dimensions." Cell 95: 431-437.
Taylor, K. A. and Glaeser, R. M. 1976. "Electron microscopy of frozen hydrated biological specimens." J Ultrastruct Res 55: 448-456.
Tolskaya, E. A., Romanova, L. I., Kolesnikova, M. S., Ivannikova, T. A., Smirnova, E. A., Raikhlin, N. T. and Agol, V. I. 1995. "Apoptosis-inducing and apoptosis-preventing functions of poliovirus." J Virol 69: 1181-1189.
Topf, M. and Sali, A. 2005. "Combining electron microscopy and comparative protein structure modeling." Curr Opin Struct Biol 15: 578-585.
Topf, M., Lasker, K., Webb, B., Wolfson, H., Chiu, W. and Sali, A. 2008. "Protein structure fitting and refinement guided by cryo-EM density." Structure 16: 295-307.
Toropova, K., Stockley, P. G. and Ranson, N. A. 2011. "Visualising a viral RNA genome poised for release from its receptor complex." J Mol Biol 408: 408-419.
Toropova, K., Basnak, G., Twarock, R., Stockley, P. G. and Ranson, N. A. 2008. "The three-dimensional structure of genomic RNA in bacteriophage MS2: implications for assembly." J Mol Biol 375: 824-836.
Toyoshima, C. and Unwin, N. 1988. "Contrast transfer for frozen-hydrated specimens: determination from pairs of defocused images." Ultramicroscopy 25: 279-291.
Tuerk, C. and Gold, L. 1990. "Systematic evolution of ligands by exponential enrichment: RNA ligands to bacteriophage T4 DNA polymerase." Science 249: 505-510.
Tuschall, D. M., Hiebert, E. and Flanegan, J. B. 1982. "Poliovirus RNA-dependent RNA polymerase synthesizes full-length copies of poliovirion RNA, cellular mRNA, and several plant virus RNAs in vitro." J Virol 44: 209-216.

Tuthill, T. J., Bubeck, D., Rowlands, D. J. and Hogle, J. M. 2006. "Characterization of early steps in the poliovirus infection process: receptor-decorated liposomes induce conversion of the virus to membrane-anchored entry-intermediate particles." J Virol 80: 172-180.
Valegard, K., Liljas, L., Fridborg, K. and Unge, T. 1990. "The three-dimensional structure of the bacterial virus MS2." Nature 345: 36-41.
Valegard, K., Murray, J. B., Stockley, P. G., Stonehouse, N. J. and Liljas, L. 1994. "Crystal structure of an RNA bacteriophage coat protein-operator complex." Nature 371: 623-626.
Valegard, K., Murray, J. B., Stonehouse, N. J., van den Worm, S., Stockley, P. G. and Liljas, L. 1997. "The three-dimensional structures of two complexes between recombinant MS2 capsids and RNA operator fragments reveal sequence-specific protein-RNA interactions." J Mol Biol 270: 724-738.
van den Worm, S. H., Stonehouse, N. J., Valegard, K., Murray, J. B., Walton, C., Fridborg, K., Stockley, P. G. and Liljas, L. 1998. "Crystal structures of MS2 coat protein mutants in complex with wild-type RNA operator fragments." Nucleic Acids Res 26: 1345-1351.
Van Dyke, T. A., Rickles, R. J. and Flanegan, J. B. 1982. "Genome-length copies of poliovirion RNA are synthesized in vitro by the poliovirus RNA-dependent RNA polymerase." J Biol Chem 257: 4610-4617.
Van Heel, M. 1987. "Angular reconstitution: a posteriori assignment of projection directions for 3D reconstruction." Ultramicroscopy 21: 111-123.
Wang, X., Peng, W., Ren, J., Hu, Z., Xu, J., Lou, Z., Li, X., Yin, W., Shen, X., Porta, C., Walter, T. S., Evans, G., Axford, D., Owen, R., Rowlands, D. J., Wang, J., Stuart, D. I., Fry, E. E. and Rao, Z. 2012. "A sensor-adaptor mechanism for enterovirus uncoating from structures of EV71." Nat Struct Mol Biol 19: 424-429.
Veesler, D., Campbell, M. G., Cheng, A., Fu, C. Y., Murez, Z., Johnson, J. E., Potter, C. S. and Carragher, B. 2013. "Maximizing the potential of electron cryomicroscopy data collected using direct detectors." J Struct Biol 184: 193-202.
Verboon-Maciolek, M. A., Krediet, T. G., van Loon, A. M., Kaan, J., Galama, J. M., Gerards, L. J. and Fleer, A. 2002. "Epidemiological survey of neonatal non-polio enterovirus infection in the Netherlands." J Med Virol 66: 241-245.
Verlinden, Y., Cuconati, A., Wimmer, E. and Rombaut, B. 2000. "Cell-free synthesis of poliovirus: 14S subunits are the key intermediates in the encapsidation of poliovirus RNA." J Gen Virol 81: 2751-2754.
Westerhuis, B. M., Jonker, S. C., Mattao, S., Benschop, K. S. and Wolthers, K. C. 2013. "Growth characteristics of human parechovirus 1 to 6 on different cell lines and cross- neutralization of human parechovirus antibodies: a comparison of the cytopathic effect and real time PCR." Virol J 10: 146.
Whitton, J. L., Cornell, C. T. and Feuer, R. 2005. "Host and virus determinants of picornavirus pathogenesis and tropism." Nat Rev Microbiol 3: 765-776.
Wigand, R. and Sabin, A. B. 1961. "Properties of ECHO types 22, 23 and 24 viruses." Arch Gesamte Virusforsch 11: 224-247.

Williams, C. H., Kajander, T., Hyypiä, T., Jackson, T., Sheppard, D. and Stanway, G. 2004. "Integrin alpha v beta 6 is an RGD-dependent receptor for coxsackievirus A9." J Virol 78: 6967-6973.
Wolf, M., Garcea, R. L., Grigorieff, N. and Harrison, S. C. 2010. "Subunit interactions in bovine papillomavirus." Proc Natl Acad Sci U S A 107: 6298-6303.
Xiao, C., Bator-Kelly, C. M., Rieder, E., Chipman, P. R., Craig, A., Kuhn, R. J., Wimmer, E. and Rossmann, M. G. 2005. "The crystal structure of coxsackievirus A21 and its interaction with ICAM-1." Structure 13: 1019-1033.
Xiao, C., Bator, C. M., Bowman, V. D., Rieder, E., He, Y., Hebert, B., Bella, J., Baker, T. S., Wimmer, E., Kuhn, R. J. and Rossmann, M. G. 2001. "Interaction of coxsackievirus A21 with its cellular receptor, ICAM-1." J Virol 75: 2444-2451.
Xing, L., Huhtala, M., Pietiainen, V., Kapyla, J., Vuorinen, K., Marjomäki, V., Heino, J., Johnson, M. S., Hyypiä, T. and Cheng, R. H. 2004. "Structural and functional analysis of integrin alpha2I domain interaction with echovirus 1." J Biol Chem 279: 11632-11638.
Yamashita, T., Sakae, K., Tsuzuki, H., Suzuki, Y., Ishikawa, N., Takeda, N., Miyamura, T. and Yamazaki, S. 1998. "Complete nucleotide sequence and genetic organization of Aichi virus, a distinct member of the Picornaviridae associated with acute gastroenteritis in humans." J Virol 72: 8408-8412.
Yamayoshi, S., Yamashita, Y., Li, J., Hanagata, N., Minowa, T., Takemura, T. and Koike, S. 2009. "Scavenger receptor B2 is a cellular receptor for enterovirus 71." Nat Med 15: 798-801.
Yamayoshi, S., Iizuka, S., Yamashita, T., Minagawa, H., Mizuta, K., Okamoto, M., Nishimura, H., Sanjoh, K., Katsushima, N., Itagaki, T., Nagai, Y., Fujii, K. and Koike, S. 2012. "Human SCARB2-dependent infection by coxsackievirus A7, A14, and A16 and enterovirus 71." J Virol 86: 5686-5696.
Yan, X., Dryden, K. A., Tang, J. and Baker, T. S. 2007. "Ab initio random model method facilitates 3D reconstruction of icosahedral particles." J Struct Biol 157: 211-225.
Ylä-Pelto, J., Koskinen, S., Karelehto, E., Sittig, E., Roivainen, M., Hyypiä, T. and Susi, P. 2013. "Complete genome sequences of three strains of coxsackievirus a7." Genome Announc 1: e0014613.
Yun, H., Kim, S., Lee, H., Byun, K. S., Kwon, S. Y., Yim, H. J., Lim, Y. S., Jeong, S. H. and Jee, Y. 2008. "Genetic analysis of HAV strains isolated from patients with acute hepatitis in Korea, 2005-2006." J Med Virol 80: 777-784.
Zhang, P., Mueller, S., Morais, M. C., Bator, C. M., Bowman, V. D., Hafenstein, S., Wimmer, E. and Rossmann, M. G. 2008a. "Crystal structure of CD155 and electron microscopic studies of its complexes with polioviruses." Proc Natl Acad Sci U S A 105: 18284-18289.
Zhang, X., Jin, L., Fang, Q., Hui, W. H. and Zhou, Z. H. 2010. "3.3 Å cryo-EM structure of a nonenveloped virus reveals a priming mechanism for cell entry." Cell 141: 472-482.

Zhang, X., Settembre, E., Xu, C., Dormitzer, P. R., Bellamy, R., Harrison, S. C. and Grigorieff, N. 2008b. "Near-atomic resolution using electron cryomicroscopy and single-particle reconstruction." Proc Natl Acad Sci U S A 105: 1867-1872.
Zhang, X., Ge, P., Yu, X., Brannan, J. M., Bi, G., Zhang, Q., Schein, S. and Zhou, Z. H. 2013. "Cryo-EM structure of the mature dengue virus at 3.5-Å resolution." Nat Struct Mol Biol 20: 105-110.
Zhu, J., Luo, B. H., Xiao, T., Zhang, C., Nishida, N. and Springer, T. A. 2008. "Structure of a complete integrin ectodomain in a physiologic resting state and activation and deactivation by applied forces." Mol Cell 32: 849-861.
Zimmern, D. and Butler, P. J. 1977. "The isolation of tobacco mosaic virus RNA fragments containing the origin for viral assembly." Cell 11: 455-462.
Zuker, M. 2003. "Mfold web server for nucleic acid folding and hybridization prediction." Nucleic Acids Res 31: 3406-3415.